DR. CATHERINE M. HULSHOF (Orcid ID : 0000-0002-2200-8076)
DR. CAMILA PIZANO (Orcid ID : 0000-0003-4124-1348)
DR. NAOMI B SCHWARTZ (Orcid ID : 0000-0002-3439-2888)
DR. SKIP J VAN BLOEM (Orcid ID : 0000-0001-7165-6646)

Article type : Article

Journal: Ecological Monographs
Manuscript type: Article

Running head: Biogeochemistry in tropical dry forests

Soil biogeochemistry across Central and South American tropical dry forests

Bonnie G. Waring,[1,2] Mark E. De Guzman,[3] Dan V. Du,[4] Juan M. Dupuy,[5] Maga Gei,[3] Jessica Gutknecht,[6] Catherine Hulshof,[7] Nicolas Jelinski,[6] Andrew J. Margenot,[8] David Medvigy,[9] Camila Pizano,[10] Beatriz Salgado-Negret[11], Naomi B. Schwartz[12], Annette M. Trierweiler,[9] Skip J. Van Bloem,[13] German Vargas G.,[3] and Jennifer S. Powers[3*]

1 Utah State University, Department of Biology and Ecology Center, Logan UT 84321, USA
2 Current address: Grantham Institute on Climate Change and the Environment, Imperial College London, United Kingdom
3 University of Minnesota, Ecology, Evolution and Behavior and Plant Sciences, St. Paul MN 55108, USA
4 University of Idaho, Department of Soil & Water Systems, Moscow ID 83844, USA

5 Centro de Investigación Científica de Yucatán, Unidad de Recursos Naturales, Mérida, Yucatán, México
6 University of Minnesota, Department of Soil, Water, and Climate, St. Paul MN 55108, USA
7 Virginia Commonwealth University, Department of Biology, Richmond, VA 23284, USA
8 University of Illinois Urbana-Champaign, Department of Crop Sciences, Urbana IL 61801, USA
9 University of Notre Dame, Department of Biological Sciences, Notre Dame IN 46556, USA
10 Universidad Icesi, Departamento de Ciencias Biológicas, Cali, Colombia
11 Universidad Nacional de Colombia, Departamento de Biología, Bogotá, Colombia
12 Dept. of Geography, University of British Columbia, Vancouver, Canada
13 Clemson University, Baruch Institute of Coastal Ecology and Forest Science, Georgetown SC, 29634, USA

*Corresponding author. E-mail: powers@umn.edu

Manuscript received 29 October 2020; accepted 2 February 2021; final version received 21 March 2021.

Abstract

The availability of nitrogen (N) and phosphorus (P) controls the flow of carbon (C) among plants, soils, and the atmosphere, thereby shaping terrestrial ecosystem responses to global change. Soil C, N, and P cycles are linked by drivers operating at multiple spatial and temporal scales: landscape-level variation in macroclimate and soil geochemistry; stand-scale heterogeneity in forest composition; and microbial community dynamics at the soil pore scale. Yet in many biomes, we do not know at which scales most of the biogeochemical variation emerges, nor which processes drive cross-scale feedbacks. Here, we examined the drivers and spatial/temporal scales of variation in soil biogeochemistry across four tropical dry forests spanning steep environmental gradients. To do so, we quantified soil C, N, and P pools, extracellular enzyme activities, and microbial community structure across wet and dry seasons in sixteen plots located in Colombia, Costa Rica, Mexico, and Puerto Rico.

Soil biogeochemistry exhibited marked heterogeneity across the sixteen plots, with total organic C, N, and P pools varying four-fold, and inorganic nutrient pools by an order of magnitude. Most soil characteristics changed more across space (i.e., among sites and plots) than over time (between dry and wet season samplings). We observed stoichiometric decoupling among C, N, and P cycles, which may reflect their divergent biogeochemical drivers. Organic C and N pool sizes were positively correlated with the relative abundance of ectomycorrhizal trees and legumes. By contrast, the distribution of soil P pools was driven by soil geochemistry, with larger inorganic P pools in soils with P-rich parent material.

Most earth system models assume that soils within a texture class operate similarly, and ignore sub-grid cell variation in soil properties. Here we reveal that soil nutrient pools and fluxes exhibit as much variation among four Neotropical dry forests as is observed across terrestrial ecosystems at the global scale. Soil biogeochemical patterns are driven not only by regional differences in soil parent material and climate, but also by local-scale variation in plant and microbial communities. Thus, the biogeochemical patterns we observed across the Neotropical dry forest biome challenge representation of soil processes in ecosystem models.

Keywords: carbon, nitrogen, phosphorus, spatial scale, seasonality, stoichiometry, tropical dry forest

1. Introduction

Interactions among carbon (C), nitrogen (N), and phosphorus (P) cycles govern terrestrial ecosystem responses to global change. The size of the plant C sink is constrained by the availability of nutrients to support growth (Wieder et al 2015). Nutrients also influence soil microbes, which regulate the size of the soil C pool through their dual roles in soil organic matter formation and loss (Liang et al. 2017). Because nutrients simultaneously stimulate ecosystem C gain (photosynthesis) and loss (decomposition), changes in nutrient supply rates may have non-linear effects on the size of the terrestrial C sink (Sistla and Schimel 2012). Moreover, nutrients interact with other global change drivers, including elevated CO_2 (Terrer et al. 2019), warming (Peñuelas et al. 2017), and altered precipitation (Rentería and Jaramillo 2011; Waring et al 2019), to control C uptake and turnover

within plants and soil. Therefore, to predict carbon-climate feedbacks, we require a mechanistic understanding of carbon-nutrient interactions in soils.

Predicted changes in the size of plant and soil C sinks are extremely sensitive to the ways in which nutrient limitation is represented in terrestrial ecosystem models (Zhu et al. 2016, Friedlingstein et al. 2014). To accurately predict belowground responses to climate change, models must capture the relationships between soil biogeochemical cycles and their primary environmental drivers: variation in climate, soil physical and chemical properties, and plant community composition. Studying C, N, and P cycles along single-factor gradients (e.g. the Long Substrate Age Gradient in Hawaii) has been fundamental to our understanding of these relationships. Yet while such gradients are a powerful experimental tool to identify the mechanisms by which individual ecosystem state factors affect C, N, and P cycling, they cannot reveal the *relative* importance of the multiple environmental drivers that structure ecosystems – information which is critical to large-scale modeling efforts. Moreover, influence of these factors on biogeochemical processes may vary depending upon the scale at which they are examined (Bradford et al. 2014). Empiricists have long recognized that soil processes, properties, and dynamics vary across a range of spatial scales, from a few centimeters to continental scales (Robertson et al. 1997; Ettema and Wardle, 2002; Zinke 1962), as well as over time. However, representing biogeochemical processes across multiple spatial scales remains a primary challenge for terrestrial ecosystem models (Campbell and Paustian 2015).

1.A *Biogeochemical processes across scales: tropical dry forests as a case study*

The challenges of predicting biogeochemical pattern and process across scales are exemplified by the climatically variable, geologically complex, and biodiverse tropical dry forest (TDF) biome. TDFs, which once occupied over 40% of forested tropical ecosystems, are characterized by warm temperatures and strongly seasonal precipitation, with at least two to three very dry months (Murphy and Lugo 1986). They also exhibit high taxonomic and functional plant diversity; TDF tree species vary in leaf habit, leaf and wood economic spectrum traits, and mycorrhizal association (Eamus 1999, Banda et al. 2016, Allen et al. 2017). Although soil nutrient cycling in TDF is under-studied in comparison with both temperate forests and their wet and moist tropical forest counterparts (Gei and Powers 2014), seasonal tropical forests play a major role in regulating global biogeochemical cycles

and their feedbacks to global change. Tropical forests dominate terrestrial C exchange with the atmosphere (Cleveland et al. 2011) and are global hotspots of biological N fixation and export (Bai et al. 2012). In seasonally dry tropical forests, these ecosystem processes are highly sensitive to ongoing changes in rainfall patterns across the biome (Allen et al. 2017), with unknown consequences for the global terrestrial C sink.

The biogeochemical heterogeneity of TDF exemplifies within-biome variation in ecosystem processes across multiple spatial and temporal scales. Although TDFs all exhibit warm temperatures, they exhibit broad variation in mean annual precipitation (from 250 to 2000 mm; Murphy and Lugo 1986) and the intensity of wet-dry season transitions (Allen et al 2017). Some TDFs have higher mean annual precipitation than evergreen moist forests, but experience months-long dry seasons without any rainfall; meanwhile, other TDFs are characterized by low annual rainfall that is more evenly spread throughout the year. Few studies have explicitly quantified this within-biome climatic variability and its effects on belowground processes. However, evidence suggests that the relative availability of N and P is sensitive to gradients of MAP, with 'leakier' soil N cycles intensifying N limitation in the drier TDFs (Campo 2016). Moreover, the intensity and duration of dry seasons strongly shapes intra-annual variability in nutrient cycling, which in turn may affect ecosystem-scale nutrient retention and loss. Dry-wet season transitions are accompanied by pulses of soil respiration (Verduzco et al. 2015) and nutrient mineralization (Singh et al. 1989; Calvo-Rodriguez et al, 2020). The size of these pulses is sensitive to the magnitude of change in soil moisture (Lado-Monserrat et al. 2014); however, no studies have investigated the magnitude of seasonal changes in TDF biogeochemistry and whether these patterns are consistent across spatial scales.

Like their wet tropical forest counterparts, TDFs also exhibit pronounced fine-scale heterogeneity in edaphic properties (Townsend et al. 2007, Waring et al. 2016). TDFs capture enormous variability in the composition of soil parent material, ranging from volcanic tuff to limestone to granite (e.g. Lugo et al. 2006, Cotler and Ortega-Larrocea 2006, Powers et al. 2009a). The geology of a site strongly influences ecosystem biogeochemistry by determining the supply of mineral-derived nutrients that are essential for plant and microbial growth (Anderson 1988). The relative availabilities of these elements may be further influenced by the extent of soil weathering, which in turn is sensitive to topography (Weintraub et al. 2015), climate (West et al. 2005), and geologic time (Chadwick et al,

1999). As soils weather and age, the bioavailability of rock-derived cations such as P tend to decrease as they are lost via leaching or occlusion; meanwhile, N availability accumulates over time via biological fixation (Walker and Syers 1976). Thus, the relative intensity of N vs. P limitation in TDF is likely sensitive to multiple interacting factors: soil parent material, the degree of rainfall-related leaching, topographic variation in weathering intensity, and the sources of ecosystem nutrient inputs (Campo 2016). Together, these drivers can generate large biogeochemical heterogeneity at relatively fine spatial scales in TDF (Pulla et al. 2016).

Although parent material is the ultimate source of rock-derived nutrients, a forest's biota mediates the biological fixation of C and N, and shapes internal cycling of macro- and micronutrients. The quantity and chemical quality of organic matter inputs to soils hinges on the composition and functional trait distributions of local tree communities. Plant communities in TDF are highly diverse (Murphy and Lugo 1986), exhibiting pronounced interspecific variation in tissue nutrient concentrations (Powers and Tiffin 2010), nutrient uptake and use efficiencies (Waring et al. 2015), and leaf and root functional traits and morphology (Hulshof and Swenson 2010, Smith-Martin et al 2019). Patterns of C and nutrient cycling may be particularly sensitive to the relative abundance of two important plant functional groups in TDFs: legumes and ectomycorrhizal trees. Many species in the superfamily Leguminosae associate with nitrogen-fixing rhizobial bacteria, and symbiotic nitrogen fixation represents a major ecosystem N input in tropical forests (Sullivan et al 2014). Soil N cycling is also strongly affected by trees that associate with ectomycorrhizal fungi, which provide their plant hosts with nutrients in exchange for photosynthate. Unlike the arbuscular mycorrhizal fungi that tend to dominate in many lowland Neotropical forests, ectomycorrhizae have some saprophytic capacity and can acquire nitrogen in organic forms (Shah et al. 2016). By competing with free-living saprotrophs, ectomycorrhizae tend to suppress rates of decomposition and slow soil nitrogen cycling (Orwin et al. 2011, Averill and Hawkes 2016, Fernandez and Kennedy 2016). Thus, the distribution of plant functional groups can create a small-scale mosaic of nutrient cycling hotspots and cold spots within a forest stand (Waring et al. 2015).

Free-living soil microbial communities also play a dominant role in driving soil biogeochemical cycles, as the stoichiometry of the microbial biomass determines relative rates of soil C, N, and P cycling (Camenzind et al. 2018). Limiting nutrients are immobilized in the microbial

biomass, whereas elements supplied in excess of demand are mineralized and potentially lost from the ecosystem via CO_2 respiration, leaching, or denitrification. C:N:P ratios of the microbial biomass are relatively constrained when compared to the degree of stoichiometric variation in plant litter and soil organic matter (Cleveland and Liptzin 2007). One way that soil microorganisms can maintain stoichiometric homeostasis is by altering investment in the different extracellular enzymes that liberate C, N, and P from organic matter (Sinsabaugh and Follstad Shah 2012). However, the microbial biomass can also exhibit stoichiometric plasticity, which is likely mediated by shifts in community composition. For example, fungi tend to have higher biomass C:N than bacteria; thus, shifts in the fungal to bacterial ratio (F:B) are often observed along gradients of soil N availability (Waring et al. 2013). Microbial biomass C:P may reflect the relative abundance of fast-growing copiotrophic organisms vs. slow-growing oligotrophs, as the former tend to build more P-rich ribosomes (Elser et al. 1996, Hartman and Richardson 2013). Because microbial community structure and abundance vary within the soil pore space and with proximity to plant roots, 'hot spots' and 'hot moments' of biogeochemical cycling emerge at fine spatial scales (Kuzyakov and Blagodatskaya 2015).

Soil biogeochemical patterns are highly heterogeneous across seasonally dry tropical forests because they can exhibit variation in each of the major soil forming-factors at relatively fine spatial grains. Our understanding of belowground nutrient cycling in TDF is further complicated by cross-scale interactions among these drivers. For instance, a regional climate envelope may encompass landscape-scale geological gradients of soil parent materials with different elemental composition and patterns of weathering (Hulshof and Powers, 2019). In turn, these edaphic gradients may select for plant communities with distinct taxonomic composition and therefore different functional traits. For example, in the TDFs of northwestern Costa Rica, oak-dominated forests growing on shallow, rocky, nutrient-poor pumice-derived soils occur in close proximity to more diverse, deciduous tree communities on richer, deeper soils (Powers et al. 2009a). The dominance of ectomycorrhizal oaks further modifies soil biogeochemistry, slowing rates of decomposition (Schilling et al. 2016) and soil nitrogen cycling (Waring et al. 2016). As a result, forests experiencing identical climate regimes can exhibit dramatically different patterns of soil biogeochemistry (Waring et al. 2016). Such observations challenge the core assumptions of Earth system models, which presume that individual ecosystems

belonging to the same biome operate in similar ways. However, as the examples above illustrate, complex interactions among climate, soil parent material, plants, and microbial communities generate a broad spectrum of variation in soil biogeochemical properties at local to regional scales. Capturing this sub-gridcell heterogeneity and its drivers remains a major challenge for ecosystem models (Medvigy et al. 2019).

1.B Experimental aims and overview

In this paper, we quantify variation in soil biogeochemistry across the Neotropical TDF biome as a case study in the drivers of C, N, and P cycling across scales. We sampled soils from sixteen forest dynamics plots in Colombia, Costa Rica, Mexico, and Puerto Rico to capture regional variation in climate regime, soil parent material, and plant community structure. Rather than seeking to isolate a single biogeochemical driver (e.g. rainfall) while holding others constant, our approach embraces the pronounced climatic, edaphic, and biotic heterogeneity that characterizes Neotropical dry forest, allowing us to assess the relative importance of these different factors. To examine local variation in soil biogeochemistry through space and time, we employed a hierarchical sampling design, replicating our measurements across multiple sampling points within plots, multiple plots within each site, and between wet and dry seasons. This sampling design allowed us to compare the magnitude of biogeochemical variation at continental (10^3 km), landscape (10^1 km), and local (10^{-2} km) scales, as well as assess the relative extent of spatial vs. temporal variation.

Our analysis was structured to target three specific research aims. The first goal (**Aim 1**) was to identify the spatial scales over which different soil biogeochemical parameters exhibit the greatest degree of variation, and to compare the magnitudes of spatial and temporal variation. The second objective (**Aim 2**) was to identify the degree to which C, N, and P cycles are linked vs. decoupled across space and time. The final goal (**Aim 3**) was to identify the drivers of the biogeochemical patterns documented in Aims 1 and 2, quantifying the relative importance of soil elemental composition, climatic regime, and biota in shaping soil biogeochemical patterns within and across the Neotropical dry forest biome. Taken together, we expect these analyses to illuminate the magnitude of biogeochemical heterogeneity within the TDF biome, the spatial scale over which this variability manifests, and the drivers of cross-scale variation in C, N, and P cycles.

2. Methods

2.A Study sites

Soils were sampled from four sites in Colombia (5.06° N, 74.83° W), Costa Rica (10.72 N, 85.59 W), Mexico (21.02° N, 89.59° W), and Puerto Rico (17.97° N, 66.87° W) (**Table 1**), with four replicate plots established within each site. The 16 plots capture dramatic gradients of mean annual precipitation, dry season length, plant community structure, and soil properties that are characteristic of the Neotropical TDF biome. Each of the four sites represents a distinct dry forest floristic group identified by Banda et al. (2016). While forest age varies among sites and plots (**Table 1**), all forests are intermediate to mature secondary forests recovering from some form of managed land use. Slopes of all plots were fairly level and plots were located within 4 km of each other or closer at all sites. Within each plot, all stems ≥2.5 cm in diameter breast height (DBH) were measured and identified to species. To situate our sites within the context of other Neotropical dry forests, we accessed a global geographic database of soil properties, ISRIC SoilGrids (https://soilgrids.org/) (**Appendix S1: Figure S1**). ISRIC grids for soil texture variables (sand, silt, and clay), pH, and cation exchange capacity (CEC) were downloaded at 0.1 degree resolution and masked the extent of all Neotropical TDF, defined as tropical and subtropical dry broadleaf forests in Olson et al. (2001). We then compared these values to values measured at our sites. Because we did not measure CEC from our soil samples, we extracted the values at our sites from the Soilgrids database.

Within each plot, we established sampling points every 5 m along a 20 m transect down the plot midline. At each 5 m marker, we collected 4 to 6 soil cores from the top 10 cm of mineral soil using a 2.5 cm diameter soil sampler and composited them. Thus, we analyzed five unique soil samples within each plot. Samplings were repeated twice in each plot: once in the wetter portion of the year (October 2016) and once in the drier portion (February 2017). With five cores per plot obtained in each season, we analyzed 160 independent soil samples in total. All soils were processed for the biogeochemical measurements described below within a week of collection. For some of the more dynamic soil properties that we measured (e.g. NO_3 concentrations), it is desirable to measure these within hours of extracting soil cores. However, this was not possible given the logistics of where our study sites are located. Thus, even though all samples were treated identically and quickly once

they arrived in the lab, we acknowledge that this may affect some of our results. Sequential P fractionations were performed only for samples collected in the dry season, whereas soil pH, texture, total C and N pools, and ammonium oxalate and citrate dithionate-extractable nutrient pools were quantified for soils collected in the wet season only. All other variables were measured on samples collected in both seasons.

2.B Biogeochemical analyses

2.B.1. Soil physicochemical properties

Soil pH for mineral samples was determined in slurries of air-dried soil and water (pH_{H2O}) with a 1:2.5 soil to solution ratio (Soil Survey Staff, 2014). Samples for textural analysis were air-dried, passed through a 2-mm sieve, and hand homogenized prior to subsampling. We then obtained three 0.5 g subsamples which were shaken overnight in 0.5% sodium hexametaphosphate and 0.5% sodium hypochlorite prior to standard analysis on a Malvern Mastersizer 3000 (Miller and Schaetzl, 2012). We ran extensive in-house validation on known size fractions of sand, silt and clay to optimize our laser particle size data for comparison with the more traditional hydrometer method (Konert and Vandenberghe, 1997). We did not pre-treat samples to remove iron oxides, and data should therefore be interpreted as 'effective' particle size distribution.

Total elemental concentrations of Al, Ca, Fe, K, P, S, and Si were quantified by X-Ray Fluorescence (XRF), using an Olympus Delta P4000EX portable XRF (pXRF) instrument (Olympus, Inc) equipped with a silicon drift detector. During analysis, the instrument was mounted in a Innov-X System Stand for stability and operated remotely through a computer console. We operated the instrument in the "mining" mode, which uses the fundamental parameters approach to correct the measured X-rays for a variety of physical phenomena (e.g., absorption and fluorescence, attenuation from incoherent scattering and the photoelectric effect, and differences in characteristic X-ray intensities). Measuring the elements of interest used three proprietary, built-in X-ray filters. The detection limit for these analyses is ~500 µg g^{-1} mg total P, with a resolution of approximately 10 µg g^{-1}, which may constrain our ability to quantify low P soils. However, previous work has shown that P measured by pXRF instruments is well correlated with wet chemical extractions (Frahm et al., 2016).

Pools of Al, Mn, and P associated with the total "free" iron (iron not contained in the crystal structures of soil minerals, but as amorphous or crystalline iron oxyhydroxides) and pools of P associated with organic molecules, amorphous or paracrystalline minerals and nano-crystalline Al, Fe, and Mn (pedogenically active iron) were determined by selective dissolutions using citrate dithionite (CD; Jackson et al., 1986) and ammonium oxalate (Soil Survey Staff, 2014, Schwertmann and Taylor, 1989). The CD extraction utilized 0.5 g of soil extracted for 12 hours in 0.4 g sodium dithionite, 0.57M sodium citrate, and deionized water (Soil Survey Staff, 2014), while the ammonium oxalate extraction utilized 0.5 g of soil extracted under dark conditions for 12 hours in 0.2M ammonium oxalate (Soil Survey Staff, 2014).

2.B.2. C, N, and P pools

Following inorganic carbon removal with sulfurous acid, total organic carbon and nitrogen were quantified on each sample with a Costech Elemental Analyzer. Sequential fractionation based on Hedley et al (1982) as modified by Margenot et al. (2017) was used to quantify seven pools of soil phosphorus. There are a number of methods to quantify "available" soil P, the choice of which depends on soil characteristics like pH. However, these metrics are agronomic predictors of crop response to P inputs. Thus, we employed sequential fractionation to all our soils, rather than tailor the extractions to each soil, to facilitate comparisons among sites. This procedure isolated four inorganic P pools: anion-exchange membrane P ($P_{i\text{-}AEM}$), an index of-bioavailable P; weakly surface-sorbed inorganic P extracted with sodium bicarbonate ($P_{i\text{-}NaHCO3}$); strongly surface-sorbed (Fe- and Al-bound) inorganic P extracted with sodium hydroxide ($P_{i\text{-}NaOH}$); and calcium P, often interpreted as apatite but also inclusive of secondary calcium phosphates (Gu et al., 2020), extracted with hydrochloric acid ($P_{i\text{-}HCl}$) (Cross and Schlesinger 1995). Three organic P pools were also quantified: water-extractable organic P ($P_{o\text{-}H2O}$); sodium bicarbonate-extractable organic P ($P_{o\text{-}NaHCO3}$), and sodium hydroxide-extractable organic P ($P_{o\text{-}NaOH}$). From these data, we estimated a labile P index (P_{labile}) by summing $P_{i\text{-}AEM}$ and $P_{i\text{-}NaHCO3}$; we also calculated organic P (P_{org}) as the sum of $P_{o\text{-}H2O}$, $P_{o\text{-}NaHCO3}$, and $P_{o\text{-}NaOH}$.

Pools of inorganic N were measured via extraction with 2 M KCl (Keeney and Nelson 1987), and NH_4 and NO_3 in these extracts were determined colorimetrically with standard methods described in Waring et al. (2016). Inorganic N was quantified for field-fresh samples and again after a two-week incubation in the laboratory to determine rates of net N mineralization. For these incubations, ~10 to

25 g field moist soils were placed in jars, covered with cling wrap, and incubated at ambient lab temperatures (~24 °C) in the dark. Over the course of the 2 weeks, every 3-4 days the jars were weighed and soils were brought back up to ambient soil moisture at time of collection by adding deionized water with a pipette. Finally, pools of C, N, and P in the microbial biomass were quantified via chloroform fumigation and direct extraction, using 0.5 M K_2SO_4 as the extractant for microbial biomass C and N (Brookes et al. 1985) and 0.5 M $NaHCO_3$ as the extractant for microbial biomass P (Brookes et al. 1982). C and N concentrations in the microbial biomass extracts were quantified on Shimadzu TOC/TN analyzer, and PO_4 content was determined colorimetrically using the ascorbic acid protocol (Murphy and Riley 1962). Organic C, organic N, and PO_4 contents of the unfumigated microbial biomass extracts were interpreted as a measure of dissolved organic carbon, nitrogen, and phosphorus availability (Waring and Powers 2016).

2.B.3. Microbial community structure and activity

Microbial community composition was examined using a modified hybrid phospholipid fatty acid (PLFA)/fatty acid methyl ester analysis (FAME) analysis (Balser et al, 2019). Briefly, 3 g of freeze-dried soil was extracted three times with chloroform, methanol, and citric acid buffer (1:2:0.9 v:v:v ratios). The chloroform liquid phase was then saponified followed by acid methylation to convert fatty-acids to fatty-acid methyl esters (FAME) before analysis on an Agilent 7890 gas chromatograph. Individual lipids were used as biomarkers to indicate broad groups within the microbial community: 16:1 ω5c for arbuscular mycorrhizal fungi; 18:1 ω9c and 18:2 ω6,9c for general fungi excluding AMF (Balser et al. 2005, Gutknecht et al. 2012); 16:1 ω7c for Gram-negative bacteria; and 15:0 iso and 17:0 iso for Gram-positive bacteria. Lipid biomass (nmol g $soil^{-1}$) was calculated by summing the abundance of all fatty acids less than or equal to 20 carbons in length. Soil fungal:bacterial ratios (F:B) were determined by summing the abundances of fungal PLFAs and dividing by the sum of bacterial PLFAs.

Finally, activities of five microbial extracellular enzymes were quantified following Saiya-Cork et al. (2002). These analyses targeted three hydrolytic enzymes: β-glucosidase (BG), which degrades cellulose; *N*-acetyl-glucosaminidase (NAG), which releases C and N from organic matter; and acid phosphatase (AP), which liberates inorganic P from organic matter. Log-transformed ratios of BG:NAG, BG:AP, NAG:AP were calculated to quantify relative microbial allocation towards the

acquisition of C:N, C:P, and N:P, respectively. Additionally, activities of two oxidative enzymes – polyphenol oxidase (PPO) and peroxidase (PER) – were measured. PPO and PER are produced by the microbial biomass to degrade recalcitrant organic matter (e.g. lignin).

2.C Statistical analyses

All statistical analyses were conducted in R version 3.3.1. To quantify how soil properties varied through space and time (**Aim 1**), we conducted nested ANOVAs to evaluate the influence of site, plot, and season (where applicable) on all biogeochemical response variables, with plot as a random factor, and modeling an interaction between site and season. These models were subject to variance partitioning to quantify the proportion of variance explained by each predictor. An analogous analysis (permutational ANOVA) was performed on the matrix of PLFA abundances using the *vegan* package (Oksanen et al. 2019), followed by a redundancy analysis to partition variation explained by climate, soil composition and weathering indices (described below), and plant community variables. Response variables were transformed as appropriate to meet assumptions of normality and heteroscedasticity. Statistical outliers were removed if Bonferroni-corrected *P* values for studentized residuals were < 0.05.

To assess linkages among C, N, and P cycles (**Aim 2**), we used Spearman's correlation analysis to examine relationships among 15 core response variables: pools of C (total organic C and microbial biomass C), N (total N, microbial biomass N, initial NH_4, and NO_3), and P (microbial biomass P, P_{labile} and $P_{organic}$), as well as enzyme activities and fungal:bacterial ratios. Similar correlation analyses were conducted to examine correspondence among C:N, C:P, and N:P ratios of soil organic matter, the microbial biomass, and enzyme activities (i.e. log-transformed ratios of BG:NAG, BG:AP, and NAG:AP). Next, the 15 core variables described above were centered and scaled prior to running a principal component analysis (PCA) to examine relationships among C, N, and P pools and fluxes.

Our final goal (**Aim 3**) was to identify the climatic, edaphic, and biotic drivers of soil biogeochemistry across scales. For these analyses, sample scores on the first and second axes of the above-mentioned PCA were interpreted as indices of C, N, and P cycling, as described further in Results. These response variables were analyzed in a multiple regression framework with the same set

of predictors: mean annual rainfall; indices of soil elemental composition and weathering; and metrics of plant community composition, productivity, and functional group composition (**Table 2**). To generate indices of soil chemical properties and weathering status, we conducted a second PCA on total elemental concentrations of Al, Ca, Fe, K, P, S, and Si in each sample, as well as the ratio of citrate-dithionite extractable Fe to total Fe (Fe_{CD}:Fe), which is correlated with weathering extent (Arduino et al 1986). In this analysis, the first principal component captured variation in the elemental composition of soils, spanning a gradient from limestone-derived soils rich in Ca and S to those with higher concentrations of Fe and Al (**Appendix S1: Figure S2**). The second principal component reflected the intensity of soil weathering. Scores on this axis were positively correlated with K, P, and Si concentrations (which are more abundant in less intensively weathered minerals) and negatively correlated with Fe_{CD}:Fe (higher values of Fe_{CD}:Fe indicate more weathering has taken place). Therefore, samples with higher scores on PC2 are likely less weathered. To summarize the effects of plant community structure on soil biogeochemistry, we included scores from the second axis of a non-metric multidimensional scaling (NMDS) analysis performed on a Bray-Curtis dissimilarity matrix of plant community composition (k=2, stress=0.00009). We also included plot-level basal area and the relative abundance of legumes and ectomycorrhizal trees. Rainfall seasonality and plant community NMDS scores along the first axis were not included in multiple regression models due to variance inflation factors > 11 (i.e. collinearity with other predictors).

Finally, we used path analysis to examine interrelationships among climate, soil composition, plant communities, and soil biogeochemistry. Our models considered the direct effects of soil parent material/weathering and plant productivity/community structure on the C, N, and P cycling indices. We also included paths linking soil characteristics with tree community composition, functional group abundance, and basal area. Climatic variables were not represented in these analyses as their inclusion decreased model fit, likely due to collinearity with other predictors. We conducted these path analyses with the *lavaan* R package (Rosseel 2012).

3. Results

3.A. Variation in climate, soil composition, and plant communities across sites

We sampled sixteen plots arrayed across four sites, which capture much of the climatic, edaphic, and floristic diversity of the Neotropical TDF biome (**Appendix S1: Figure S1**). These plots exhibited strong variation in climate and soil properties tied to parent material and weathering status (**Table 1**). Both the Colombian and Costa Rican sites experience relatively high MAP; however, rainfall seasonality is much more pronounced in Costa Rica, where plots receive almost no rain for half the year. Similarly, although both the Mexican and Puerto Rican sites are characterized by low MAP, the latter are more aseasonal, as the dry season lasts for the majority of the year. These climatic differences influenced soil water content and its variability across seasons. Despite high rainfall, Colombian soils tended to have the lowest gravimetric soil moisture in both dry and wet seasons, potentially reflecting the sandy soil texture at the site (**Table 3**; **Table 5**) and the fact that we sampled during a wet season with unusually low rainfall (Pizano, pers. obs). By contrast, soils in Costa Rica and Mexico were clay rich, had a higher dry season moisture content, and showed greater temporal variability in soil moisture (which increased over 2-fold in the wet season at both sites). Soils at the Puerto Rican site had intermediate clay content, and soil moisture was highly variable within and among plots (**Table 3; Table 5**).

The four sites also capture substantial variation in soil elemental composition and weathering status. Reflecting their recent inter-Andean origins, total concentrations of soil K and Si in the Colombian plots were 2 to 4-fold greater than those at other sites, and Colombian soils tended to be higher in total P as well. However, within-plot variability in soil P was extremely high, and therefore total P did not vary significantly among sites. Meanwhile, limestone-derived soils at the Puerto Rican sites had 8-fold greater concentrations of Ca *vs.* the other sites, and were the only soils to contain detectable quantities of S. These soils also exhibited a much more alkaline pH than soils at other sites (**Table 3; Table 4**). Finally, concentrations of Fe and Al were approximately twofold greater in the clay-rich Costa Rican and Mexican soils vs. the sandier Colombian and Puerto Rican soils. Although Al, Ca, Fe, K, Si, and S differed dramatically among sites, 2-14% of the variation in these element concentrations was observed at the plot scale, and 4-15% within a plot.

3.B. *Aim 1: Quantifying variation in soil C, N, and P pools across sites and seasons*

3.B.1. *Spatial variation in soil biogeochemistry*

For most of the soil parameters studied, over half of the observed variation occurred at the regional (10^3 km) scale, although there was also pronounced heterogeneity among and within plots. Site identity accounted for the majority of variance in total organic C, microbial biomass C, and dissolved organic C (DOC). Total organic C concentrations were four-fold higher at the Puerto Rican sites vs. the Colombian and Costa Rican sites, with intermediate values in Mexico; microbial biomass C and DOC pools showed a similar pattern (**Figure 1, Table 3, Table 5, Appendix S1: Figure S3**). Paralleling trends observed for C pools, total organic N concentrations and microbial biomass N pools exhibited most variation across sites, and were four to five times larger in Puerto Rico site vs. Colombia and Costa Rica (**Figure 1, Table 3, Table 4, Table 5, Appendix S1: Figure S3**). By contrast, dissolved organic N, NO_3 and NH_4 pools exhibited as much or more variation at the plot scale than the site scale (**Figure 2**). The ratio of NH_4:NO_3 was four times greater in Puerto Rico and Mexico vs. Colombia and Costa Rica (**Figure 1, Table 5**).

We also observed large differences among sites in dry-season P pools. Organic P pools were 40% larger in Costa Rica and Puerto Rico vs. the other sites (**Figure 1, Table 3, Table 4**). However, most of the variation in this pool occurred at the plot scale (**Figure 2**), and its composition varied greatly among sites (**Appendix S1: Figure S4**). Water-extractable P pools ($P_{o\text{-}H2O}$) were four-fold greater in Colombia and Costa Rica vs. Mexico and Puerto Rico. By contrast, $P_{o\text{-}NaHCO3}$ pools were 3 to 4-fold higher in Puerto Rico vs. the other sites. Residual organic P ($P_{o\text{-}NaOH}$) did not vary among sites. Microbial biomass P pools were four-fold larger in Colombia and Puerto Rico vs. the other sites (**Figure 1, Table 3, Table 5, Appendix S1: Figure S3**). Labile P pools (i.e., the sum of $P_{i\text{-}AEM}$ and $P_{i\text{-}NaHCO3}$) were nearly nine-fold larger in Colombia vs. the other sites (**Figure 1, Table 3, Table 4**); thus, site accounted for the majority of the variance in P_{labile} (**Figure 2**). The apatite P pool ($P_{i\text{-}HCl}$) was also 2 to 8-fold larger in Colombia relative to the other sites, whereas the occluded P pool ($P_{i\text{-}NaOH}$) was 50% smaller in Puerto Rico vs. elsewhere. Bicarbonate-extractable PO_4 (quantified in unfumigated microbial biomass P extracts) was significantly higher in Puerto Rico than all other sites (**Table 3; Table 5**).

Indices of microbial community structure and function exhibited quite strong spatial patterns. The total abundance of fungal PLFAs varied most across sites, and was 2.5 to 6-fold greater in Mexico and Puerto Rico than in Costa Rica and Colombia (**Figure 3A**), with a nearly identical pattern

observed for F:B. The composition of bacterial and fungal communities varied significantly among sites and plots (**Figure 3B, Appendix S1: Table S1**). By contrast, most of the variation in microbial extracellular enzyme activities was observed within plots (**Figure 2**). However, NAG activity was 3-fold greater in Mexico and Puerto Rico vs. Colombia and Costa Rica, and oxidative enzyme activities tended to be higher in Costa Rica and Puerto Rico than the other two sites (**Appendix S1: Figure S5**).

3.B.2. *Temporal variation in soil biogeochemistry*

Season of sampling and the interaction between season and site explained a fairly small fraction of the variance in all measured biogeochemical variables (<1 – 16% and <1-12%, respectively), as temporal changes in biogeochemistry were relatively modest. The one exception to this pattern was soil moisture, which increased dramatically in the wet season in every site but Colombia. Total elemental concentrations of Al, Ca, Fe, K, P, and Si were essentially unchanged between dry and wet seasons, but pools of organic C, N, and P were comparatively more dynamic across seasons. The size of the microbial biomass carbon pool did not vary consistently through time, increasing in the wet season in Colombia and Mexico, but decreasing in Costa Rica. However, DOC pools were approximately 20% higher in the dry vs. wet season across all sites (**Appendix S1: Figure S3**). Moreover, all labile N pools, including microbial biomass N, increased in the wet season, although the magnitude of change differed by site (**Appendix S1: Figure S3**). Net N mineralization rates increased in the wet season everywhere except Colombia, where rates declined three-fold. Both microbial biomass P pools and bicarbonate-extractable PO_4 pools were also three times larger in the wet vs. dry season. Seasonality had very little effect on microbial community structure, as season of sampling explained only 1.3% of the variance in PLFA abundance. The fungal:bacterial ratio decreased at some sites and increased in others during the wet season (**Appendix S1: Figure S3**). NAG and PPO activities generally increased in the wet season (although again, the magnitude of response differed among sites), but other enzyme activities did not vary seasonally.

3.C Aim 2: Quantifying coupling of C, N, and P cycles

Total organic C and N were strongly positively correlated to each other and to microbial biomass C, N, and P pools (**Appendix S1**: **Table S2a**), and the extracellular enzyme NAG. Meanwhile, relationships of these variables with organic and inorganic P pools were much weaker or absent.

Despite the strong correlations between C and N pool sizes, the stoichiometry of soil organic matter varied considerably across the four sites. Soil C:N was lowest in Mexico (10.5 ± 0.5) and highest in Puerto Rico (14.5 ± 0.8), with intermediate values observed in the other two sites (**Appendix S1: Figure S6**). Soil C:N ratios were unrelated to variation in microbial biomass C:N or enzyme C:N (**Appendix S1: Table S2b**). A similar decoupling among the C:P ratios of soil, microbial biomass, and enzyme activities was observed (**Appendix S1: Table S2b**), despite 3.5-fold variation in soil $C:P_{org}$ ratios across sites (ranging from 231 ± 15 in Costa Rica to 825 ± 52 in Puerto Rico). Soil $N:P_{org}$ also varied among sites (**Appendix S1: Figure S6**), was unrelated to microbial biomass N:P, and only weakly correlated to enzyme N:P (**Appendix S1: Table S2b**).

A PCA conducted on a core dataset of soil biogeochemical variables revealed that indices of C and N cycling were closely coupled with one another, and orthogonal to variation in P cycling (**Figure 4**). The variables that loaded most strongly onto the first principal component, which explained 39% of the variance in soil biogeochemistry, were total organic C and N, microbial biomass C and N, and NAG activity. Thus, scores along the first principal component axis are interpreted as an integrative index of organic C and N cycling. The second principal component, which captured 12% of the total variance, was defined by labile and microbial biomass P pools and the fungal:bacterial ratio. P_{labile} and F:B were negatively correlated ($\rho = -0.53$, $P < 0.001$). Scores along this axis therefore capture differences in soil P cycling among samples, along with variation in microbial community structure.

3.D. Aim 3: Identifying climatic, edaphic, and biotic drivers of soil biogeochemistry

Our index of C and N cycling (PC1, **Figure 4, Table 2**) was significantly related to MAP ($\beta = -1.37$, $P = 0.002$) and the abundance of both ectomycorrhizal trees ($\beta = 1.10$, $P < 0.001$) and legumes ($\beta = 0.45$, $P = 0.030$) in a multiple linear regression ($R^2 = 0.668$, **Appendix S1: Figure S7**). Path analysis (**Figure 5A, Appendix S1: Table S3**) confirmed that ectomycorrhizae and legumes shaped soil C and N cycling. This analysis also suggested that soil elemental composition and weathering affected biogeochemistry both directly and indirectly through their influence on plant community structure. Stand-level basal area had no influence on soil C and N cycling in the multiple regression or path analyses.

In a multiple regression model (R^2 =0.512), the P cycling index (PC2, **Figure 4, Table 2**) was significantly correlated with our index of soil parent material (β = -0.37, *P* = 0.024) and weathering status (β = 0.76, *P* = 0.005) (**Appendix S1: Figure S8**). A path analysis also highlighted the importance of soil weathering (**Figure 5B, Appendix S1: Table S3**), whereas plant community structure and stand basal area were unrelated to P cycling characteristics.

Controls on microbial community structure (as assessed via PLFAs) were somewhat different than those observed for C, N, and P pools. Variance partitioning conducted following a redundancy analysis suggested that MAP was the most important driver of microbial community structure (R^2_{adj} = 0.254), followed by soil chemical composition and weathering (R^2_{adj} = 0.197) and the relative abundance of legume and ectomycorrhizal trees (R^2_{adj} = 0.169).

4. Discussion

By quantifying a broad suite of biogeochemical processes at hierarchical spatial scales, we developed an unprecedentedly detailed picture of soil C, N, and P cycles in seasonally dry tropical forests. Our study captured the extreme biogeochemical heterogeneity that is characteristic of tropical forests (Townsend et al. 2008), with dramatic variation in C, N, and P pools and fluxes observed both within and among sites. Although seasonal dynamics in soil biogeochemistry were more subtle than differences observed across forests, cross-site differences in rainfall regime have likely shaped soil properties indirectly by influencing plant community structure and soil weathering.

Our findings echo broad biogeochemical patterns quantified in other seasonally dry tropical forests. As observed elsewhere (Solis and Campo 2004), the microbial biomass represents a major N and P sink, and is two to eight-fold larger than the plant-available N and P pools (except in Colombia, where the labile P pool is extremely large due to the geological context of this site). Moreover, microbial biomass nutrient pools are seasonally dynamic, suggesting that plant-microbe competition for nutrients is sensitive to the timing of rainfall events (Waring and Powers 2016, Singh et al. 1989). Additionally, the pronounced variation in the relative availability of N and P across sites is consistent with other studies that identify shifts in nutrient limitation across gradients of rainfall and stand age (Gamboa et al. 2010, Campo 2016). Below, we expand on these insights to discuss drivers of

biogeochemical patterns in tropical dry forests as a case study in the scale dependence of C, N, and P cycling.

4.1 Scale of variation in soil biogeochemical properties

Our first overall objective (**Aim 1**) was to quantify the dominant spatial scales of variation in a suite of biogeochemical pools and fluxes, including any seasonal patterns. We found that organic C and N pools tend to vary most at regional (site) scales, whereas inorganic nutrient pools exhibit substantial variability at finer spatial grains (i.e., among or within plots). Interestingly, patterns of spatial variation in soil P pools were the opposite of those observed for C and N: labile P pools vary most at the site scale, whereas organic P pools vary most among or within plots. The extremely distinctive geochemistry of the soils at the Colombian site (i.e., the very large apatite and inorganic P pools) likely account for the strong signature of site identity on P_{labile}.

In comparison with the dramatic spatial variation in soil biogeochemistry observed across plots, we found very modest temporal variation in C, N, and P cycling between seasons. In our study, the season of sampling had clear effects on soil moisture, which was higher in all sites during the wet season compared to the dry season. However, this did not translate into dramatic seasonal differences in biogeochemistry: although nutrient pools varied significantly between wet and dry periods in many cases, the magnitude of variation explained by season was generally quite small. Activities of NAG and PPO increased in the wet season, alongside microbial biomass N and P and inorganic N and P pools, suggesting that rainfall triggers an acceleration of microbial nutrient uptake and soil N and P cycling (Waring and Powers 2016). These patterns echo biogeochemical shifts observed in a seasonally dry tropical forest in India, where nutrients were immobilized by microbial biomass pools during the dry season and released in the wet season (Singh et al, 1989).

In general, the sign (if not the magnitude) of seasonal biogeochemical responses was consistent across sites, but there were a few exceptions to this pattern. Over the transition from wet to dry seasons, the size of the microbial biomass, the ratio of fungi to bacteria, and rates of net N mineralization responded in opposite directions across sites. However, these divergent responses were not related in any consistent way to rainfall regime. Other studies have shown that tree species identity influences seasonal patterns of microbial immobilization or release of nutrients (Galicia and

Garcia-Oliva 2004). Clearly, the factors regulating seasonal shifts in soil biogeochemistry are complex and difficult to generalize across forests. Thus, understanding how both long-term rainfall regimes and intra-annual variation in rainfall affect microbial dynamics and biogeochemical processes in dry forests is a high priority for future research (Calvo-Rodriguez et al 2020).

4.2 Coupling among C, N, and P cycles

Our second goal (**Aim 2**) was to examine how the distinct responses of C, N, and P cycles to climatic, edaphic, and biotic drivers link or decouple soil biogeochemical processes. Theory predicts that microbial biomass stoichiometry should be relatively homeostatic across broad environmental gradients, producing predictable linkages among C, N, and P cycles (Cleveland and Liptzin 2007, Sinsabaugh and Follstad Shah 2012), and this assumption is often embedded in ecosystem models (Achat et al. 2016). However, in our study, no stoichiometric relationships apply across the broad range of sites examined. Instead, the unique resource environment characteristic to each site shapes both microbial biomass stoichiometry and enzymatic allocation towards carbon and nutrient acquisition.

Soils in the Puerto Rico and Mexican forests are characterized by high enzymatic investment in N acquisition and elevated fungal:bacterial and NH_4:NO_3 ratios, patterns which are consistent with a conservative N cycle and (potentially) microbial N limitation. However, other N cycling parameters diverge dramatically between the two forests. Despite exhibiting the highest soil C:N ratios, the microbial biomass in the Puerto Rican plots had a lower C:N than observed anywhere else. The N-rich microbial biomass may reflect the presence of ectomycorrhizal fungi in Puerto Rican plots, where ectomycorrhizal trees were most abundant. Ectomycorrhizae can comprise up to 30% of the total microbial biomass in a typical soil (Hogberg and Hogberg 2002) and have lower biomass C:N relative to free-living decomposers (Zhang and Elser 2017). By contrast, Mexican soils showed the reverse pattern: the microbial biomass is relatively N-poor despite the low C:N ratio of soil organic matter. This could indicate a microbial biomass dominated by saprotrophic fungi, which generally have a higher biomass C:N ratio than bacteria (Waring et al. 2013, Strickland and Rousk 2010) or symbiotic fungi (Zhang and Elser 2017).

Similarly, although soils in both Costa Rica and Colombia are rich in P relative to the other sites, the sources and biogeochemical consequences of high phosphorus availability differed between them. In Colombia, apatite appears to be the dominant soil P pool, and the labile inorganic phosphorus pool is extremely large. As a result, the microbial biomass is P enriched despite a trend towards lower soil phosphatase activity than observed in any other forest. Meanwhile, organic P represents the largest phosphorus pool in Costa Rican soils. At that site, acid phosphatase and oxidative enzyme activities are elevated and biomass C:P ratios are high, suggesting microbes are allocating extracellular enzymes to counteract P limitation.

4.3 The role of ecosystem state factors in shaping soil biogeochemistry

Our final objective (**Aim 3**) was to assess the relative importance of climate, soil composition, and organisms for relative rates of C, N, and P cycling. Whereas P cycling appears to be largely dictated by soil weathering status, C and N cycling are much more sensitive to the community structure of plants and their associated root symbionts. These edaphic and biotic properties, in turn, are shaped by variation in precipitation regime across tropical dry forests.

We found that soil P pools responded most strongly to variation in soil elemental composition and weathering extent, which can influence P cycling in multiple ways. First, because soil parent material is the ultimate source of ecosystem P inputs, the geochemistry of bedrock sets an upper limit on soil P availability. Among the four sites studied here, the geologically young soils of the Colombian forest (Jungerius 1976) have the highest concentrations of total and apatite P, which are linked to larger pools of labile inorganic P. Second, as soils weather in humid climates, they become more enriched in Al and Fe oxides, which can bind P and render it unavailable for uptake (Wilson et al. 2017). This explains the relatively large recalcitrant P pools in the Fe and Al-rich soils of the Costa Rican and Mexican sites, where stronger seasonal variation in rainfall and older soil ages may promote soil weathering. By contrast, the highly organic surface soils in the Puerto Rican forest have abundant organic P, and have little Al and Fe to occlude available phosphorus (although Ca may render P less bioavailable in alkaline soils). As a result of these patterns, P concentrations in the microbial biomass are greater in Colombia and Puerto Rico than elsewhere, reflecting higher bioavailability.

In contrast with rock-derived nutrients like phosphorus, organisms drive ecosystem inputs of carbon and nitrogen; thus, patterns of C and N cycling were much more sensitive to plant community structure at each site. However, soil parent material and weathering status also play a role in shaping these cycles through both direct and indirect mechanisms. Direct impacts are likely mediated by mineralogical characteristics of the soil: the dominant types of clay minerals, the presence of iron and aluminum oxides, and base cations can all influence the strength of organo-mineral bonds that protect organic C and N from decomposition (Rasmussen et al. 2018). Soil texture and elemental composition also influence organic matter cycling indirectly by shaping plant community structure (Werden et al. 2018, John et al. 2007, Jha and Singh 1990). The diversity and taxonomic composition of plant assemblages at a particular site will dictate the chemistry of senescent leaf, wood, and root tissues, which in turn affects the belowground fate of plant-derived organic matter (Cotrufo et al. 2013). Due to the greater metabolic costs associated with decomposition of chemically complex substrates, microbial growth yields are lower on more recalcitrant plant tissues (Frey et al. 2013). Additionally, microbial C use efficiency (the proportion of C uptake that is retained in the biomass vs. respired) should be maximized under conditions of C limitation (Sinsabaugh et al. 2013), whereas N use efficiency is enhanced when N is in low supply (Mooshammer et al. 2014). Consequently, the stoichiometry and recalcitrance of organic matter inputs affects retention of C and N belowground.

Plant interactions with their microbial symbionts also exert strong control over ecosystem C and N cycling. In contrast to many other Neotropical forests where ectomycorrhizal trees form monodominant stands (Corrales et al. 2018), ectomycorrhizal trees generally occupied < 10% of basal area across these Neotropical sites. However, among the sixteen plots studied here, the highest soil organic C and N concentrations were observed in the forests where > 20% of stand basal area was occupied by ectomycorrhizal trees. Ectomycorrhizal fungi have the capacity to degrade organic matter, thereby competing directly with free-living decomposers (Shah et al. 2016). As a result, ectomycorrhizae tend to suppress rates of organic matter decomposition (Averill and Hawkes 2016, Schilling et al. 2016, McGuire et al. 2010), potentially leading to accumulation of soil C. The presence of ectomycorrhizae also shapes patterns of N cycling, leading to a more conservative nutrient economy where N cycles mostly in organic form (Phillips et al. 2013, Corrales et al. 2016).

Although they had a weaker imprint on soil biogeochemistry than did ectomycorrhizal trees, N-fixing legumes also influence C and N cycling across the four sites, likely through a variety of complementary mechanisms. First, the presence of legumes can directly affect soil nitrogen availability via symbiotic biological N fixation. However, the relationship between N fixer abundance and ecosystem N inputs is complex and difficult to predict. Tropical forest legumes can exhibit substantial interspecific variation in nodulation and fixation rates (Gei and Powers 2015, Wurzburger and Hedin 2016), and many species exhibit a facultative fixation strategy (Sheffer et al. 2015, Barron et al. 2011). In general, however, legumes have greater tissue concentrations of nitrogen than co-occurring plant species (Adams et al. 2016). As described above, the stoichiometry of organic matter inputs to soils influences microbial growth efficiency and patterns of nutrient immobilization. Moreover, in younger tropical forests recovering from disturbance, symbiotic N fixation can accelerate tree growth at the stand scale (Batterman et al. 2013), which affects the quantity of organic matter inputs to soil. This last mechanism may be of limited importance in these tropical dry forests, as we found no evidence that variation in stand-level basal area (a surrogate for plant productivity) influenced C, N, or P cycling. However, there is increasing evidence that the majority of soil organic matter is formed from roots rather than aboveground inputs (Rasse et al. 2005, Jackson et al. 2017). There are few data to constrain the spatial or temporal dynamics of belowground plant C allocation across tropical forests, although the ratio of above- to belowground biomass tends to decrease with mean annual rainfall (Waring and Powers 2017).

Each of the ecosystem state factors described above – soil weathering, plant community structure, and functional group abundance – is sensitive to climate. With only four sites, we have limited power to tease apart variation in both amount and seasonality of rainfall. Moreover, the relationship between precipitation regime and biogeochemistry is mediated by ecosystem properties which exhibit strong variation within and among sites. For example, the moisture environment experienced by soil microbes is influenced not only by rainfall, but also by soil texture, which strongly shapes the relationship between soil water content and soil water potential. Precipitation also causes nutrient leaching, although among the four sites studied here, the wettest forest happened to be situated on young, relatively unweathered soils with high total P content (Jungerius 1976), and thus a negative correlation between rainfall and P availability was not observed. Additionally, precipitation

regime influences the composition and functional trait distribution of tree communities in TDF, thereby exerting a strong indirect influence on C, N, and P cycling (Vargas et al, unpublished manuscript).

Finally, humans exert a strong influence over biogeochemical processes in all terrestrial ecosystems, especially those that are recuperating from land use change. In our study, all forests in Colombia, Costa Rica, and Mexico were regenerating from agricultural abandonment, whereas plots in Puerto Rico have been under continuous tree cover for at least a century. We do not have enough information about site histories to assess how this variability in prior land use may have impacted the soil properties measured here. However, since previous land use varies at the scale of the individual forest plot, we can use our variance decomposition to make inferences about the contribution of site history to contemporary biogeochemical patterns. Total organic C, N, and P pools exhibited 25-50% of total variance at the plot scale, suggesting that land use change impacts are potentially substantial. This is consistent with previous studies showing that land use change strongly impacts soil organic matter stocks in the tropics, although the direction and magnitude of these changes is dependent on climate and soil mineralogy (Powers et al. 2011).

4.4 Synthesis and implications for predicting the future of the tropical dry forest biome

Our analyses not only revealed tremendous heterogeneity in soil biogeochemistry across the Neotropical dry forest biome, but also uncovered relationships among ecosystem state factors that can predict this variation over space and through time. We found that C, N, and P concentrations in soil organic matter and the microbial biomass are tightly coupled to variation in soil parent material and plant community structure, factors which vary most at the site level. By contrast, inorganic nutrient pools and enzyme activities exhibit substantial variability within individual plots, likely reflecting the fine-scale heterogeneity in the microbial processes that drive nutrient mineralization. Marked variation in C, N, and P cycling observed within and among plots suggests that the effects of regional variation in climate and soil parent material are mediated through ecological processes occurring at finer spatial grains.

Moreover, our analyses show that C, N, and P cycles clearly respond to different environmental drivers, which may decouple their responses to environmental change. The cycling of rock-derived nutrients like phosphorus is closely tied to soil weathering and elemental composition,

whereas carbon and nitrogen are much more responsive to variation in plant community structure. C and N cycles are more closely intertwined with one another than with the P cycle, reflecting biochemical controls on decomposition: C and N atoms in organic matter are directly bonded to one another and are therefore mineralized together, whereas organic P is indirectly ester-bonded to C and can be biochemically mineralized separately (McGill and Cole 1981). These observations have important implications for our ability to predict ecosystem process rates under global change: if N and P cycles exhibit divergent responses to elevated CO_2 and altered climates, they will need to be modeled independently (Reed et al. 2015).

Interactions among C, N, and P cycles are increasingly represented in soil biogeochemical models (Yu et al. 2019), land surface models (Goll et al. 2017, Thum et al. 2019, Yang et al. 2019), and even earth system models (Zhu et al. 2019). Representing nutrient limitation of plant and microbial processes can change the direction and magnitude of terrestrial C sink responses to elevated CO_2 and other global change drivers (Wieder et al. 2015). However, model representations of N and P cycling processes vary considerably, and assumptions about mechanisms of plant nutrient uptake strongly influence predicted changes in the strength of tropical forest C sinks (Fleischer et al. 2019). Moreover, most earth system models represent vegetation dynamics in tropical forests with just a handful of plant functional types, neglecting variation in ecosystem function across gradients of seasonality (Oleson et al. 2013). The biogeochemical patterns and processes we observed across forests can therefore provide valuable insights on the ways in which C, N, and P cycles should be represented in earth system models - within tropical dry forests specifically and across terrestrial ecosystems more generally.

Ecosystem model predictions appear to be extremely sensitive to the flexibility of C:N:P ratios in plant and microbial biomass, and the factors that control labile P fluxes among plants and microbes (Achat et al. 2016, Fleischer et al. 2019). We observed that C:N:P ratios of the soil organic matter, microbial biomass, and extracellular enzymes were largely uncorrelated within and among sites, potentially reflecting adaptations of site-specific biota to nutrient supply rates. This suggests that modelers should not extrapolate stoichiometric ratios measured at a handful of sites to represent nutrient cycling patterns across the tropical forest biome. Moreover, given the close links between soil mineral composition and P cycling observed here, it is important to consider how plants, microbes,

and mineral surfaces might compete for labile phosphorus (Zhu et al. 2016, Yu et al. 2019). Soil parent material and weathering status play an important dual role in mediating the bioavailability of phosphorus, determining not only the magnitude of ecosystem P inputs, but also the degree to which labile P is occluded from biological uptake.

Additionally, it is evident that plant symbionts, including mycorrhizal fungi and N-fixing bacteria, play a large role in driving belowground C and N cycles. Yet these plant-microbe interactions are not usually explicitly represented in ecosystem models, even those that consider variation in plant community composition within and among biomes. Generally, plant functional types are defined by plant morphology, leaf phenology, or 'lifestyle' (e.g. woody vs. herbaceous, annual vs. perennial, or evergreen vs. deciduous groups), or by traits that directly affect photosynthetic capacity (Wullschleger et al. 2013, van Bodegom et al. 2012, Bonan et al. 2002). However, including plant-microbe symbioses in functional type definitions may be particularly critical to accurately predict ecosystem-scale biogeochemical patterns (Allen et al. 2020). This is because plant interactions with their microbial symbionts not only affect patterns of soil nutrient cycling, but also whole-plant physiology. For example, N-fixing legumes have higher leaf nitrogen content and water-use efficiency in comparison with non-fixing plants (Adams et al. 2016). Ectomycorrhizal plants appear to have slower growth rates and more conservative nutrient use strategies than arbuscular mycorrhizal species (Averill et al. 2019, Cornelissen et al. 2001). To date, efforts to incorporate N-fixing and mycorrhizal plant functional types into ecosystem models have been fairly limited. However, including N-fixing legumes in vegetation models can improve their representation of plant-soil interactions and successional dynamics in tropical forests (Medvigy et al. 2019, Levy-Varon et al. 2019). Similarly, models which explicitly represent ecological interactions between ectomycorrhizal fungi, their plant hosts, and free-living saprotrophs alter predictions of ecosystem C storage (Moore et al. 2015, Orwin et al. 2011, Sulman et al. 2017).

Finally, we observed substantial variation in C, N, and P pools and fluxes over fine spatial scales, and biogeochemical cycles often responded to cross-scale interactions among climate, plant community composition, and soil geochemistry. Models often struggle to capture relationships among ecosystem processes that are measured at different scales, from the soil pore to the forest stand (Manzoni and Porporato 2009). Most ecosystem models represent regional variation in climate as the

dominant driver of ecosystem processes, ignoring sub-grid variation in soils and plant communities which may mediate climatic effects on soil biogeochemistry (Bradford et al. 2014, Medvigy et al. 2019). Our results strongly suggest that such simplistic representations are unlikely to capture realistic variation in C, N, and P cycling through space and time.

4.5 Conclusions

The state factor model of soil development, which has influenced ecosystem ecologists for nearly eight decades, holds that "ecosystems can be defined as those portions of the earth's terrestrial surface whose properties vary in response to variations in the state factors," namely climate, soil parent material, topography, time, and biota (Amundsen and Jenny 1997, Jenny 1941). Our study reveals that all of these drivers exhibit substantial variation within a biome, generating significant biogeochemical heterogeneity at pedon to regional scales. In fact, across the four forests studied here, pools of C, N, and P in the soil organic matter and microbial biomass exhibit a similar magnitude of variation to that observed globally (Cleveland and Liptzin 2007). This variation poses a significant challenge for ecosystem models, many of which seek to reduce complexity by defining internally cohesive biomes with similar soil properties and plant functional type distributions. However, accurately capturing ecosystem responses to rising atmospheric CO_2, nutrient deposition, or warming will likely require explicit consideration of the ecological relationships among plant communities, soil microbes, and the biogeochemical processes they mediate, and how these relationships manifest over multiple spatial and temporal scales.

Acknowledgments

We thank the United States Department of Energy for funding through the research grant DE-SC0014363 for funding for this work. We thank Daniel Pérez-Aviles, Ramón Agosto Diaz, David Riverta-Polanco, and Tristan A.P. Allerton for help in the field and Sara Bauer and Jon Bertram for help in the lab. In Puerto Rico, we acknowledge PG Murphy and the International Institute of Tropical Forestry for initial site work and Eloy Martínez and Darien López of the Puerto Rico Departamento

de Recursos Naturales y Ambientales for site access. Technical Contribution No. 6841 of the Clemson University Experiment Station.

Supporting Information

Additional supporting information may be found online at: [link to be added in production]

Data Availability

Data (Waring et al. 2021) are available from the Dryad Digital Repository: https://doi.org/10.5061/dryad.v15dv41vf

Literature cited

Achat DL, Augusto L, Gallet-Budynek A, Loustau D. Future challenges in coupled C-N-P cycle models for terrestrial ecosystems under global change: a review. *Biogeochemistry*. 2016; 131:173-202

Adams MA, Turnbull TL, Sprent JI, Buchmann N. Legumes are different: Leaf nitrogen, photosynthesis, and water use efficiency. *Proceedings of the National Academy of Sciences*. 2016; 113:4098-4103

Allen K, Dupuy JM, Gei MG, et al. Will seasonally dry tropical forests be sensitive or resistant to future changes in rainfall regimes? *Environmental Research Letters*. 2017; 12:023001-023016

Allen, KE, Fisher JB, Phillips RP. Powers JS, and Brzostek ER. Modeling the carbon cost of plant nitrogen and phosphorus uptake across temperate and tropical forests. *Frontiers in Forests and Global Change* 2020; 21, https://doi.org/10.3389/ffgc.2020.00043

Amundson R, Jenny H. On a state factor model of ecosystems. *BioScience*. 1997; 47:536-543

Anderson DW. The effect of parent material and soil development on nutrient cycling in temperate ecosystems. *Biogeochemistry*. 1988; 5:71-97

Arduino E, Barberis E, Ajmone Marsan F, Zanini E, Franchini M. Iron oxides and clay minerals within profiles as indicators of soil age in Northern Italy. *Geoderma*. 1986; 37:45-55

Averill C, Hawkes CV. Ectomycorrhizal fungi slow soil carbon cycling. *Ecology Letters.* 2016; 19:937-947

Averill C, Bhatnagar JM, Dietze MC, Pearse WD, Kivlin SN. Global imprint of mycorrhizal fungi on whole-plant nutrient economics. *Proceedings of the National Academy of Sciences*. 2019; 116:23163-23168

Bai E, Houlton BZ, Wang YP. Isotopic identification of nitrogen hotspots across natural terrestrial ecosystems. *Biogeosciences.* 2012; 9:3287-3304

Balser TC, Liang C, Gutknecht JLM. Linking microbial community analysis and ecosystem studies: A rapid lipid analysis protocol for high throughput. *Soil Ecology Letters.* 2019; 1:22-32.

Balser TC, Treseder KK, Ekenler M. Using lipid analysis and hyphal length to quantify AM and saprotrophic fungal abundance along a soil chronosequence. *Soil Biology and Biochemistry*. 2005; 37: 601–604

Banda K, Delgado-Salinas A, Dexter KG, Linares-Palomino R, Oliveira A, Prado D, *et al*. Plant diversity patterns in neotropical dry forests and their conservation implications. *Science*. 2016; 353:1383-1387

Barron AR, Purves DW, Hedin LO. Facultative nitrogen fixation by canopy legumes in a lowland tropical forest. *Oecologia.* 2011; 165:511-520

Batterman S, Hedin L, van Breugel M, Ransijn J, Craven D, Hall J. Key role of symbiotic dinitrogen fixation in tropical forest secondary succession. *Nature*. 2013;502:224-227.

Bonan GB, Levis S, Kergoat L, Oleson KW. Landscapes as patches of plant functional types: An integrating concept for climate and ecosystem models. *Global Biogeochem Cy*. 2002; 16

Bradford MA, Ii RJW, Baldrian P, et al. Climate fails to predict wood decomposition at regional scales. *Nature Climate Change*. 2014; 4:625-629.

Brundrett MC. Mycorrhizal associations and other means of nutrition of vascular plants: understanding the global diversity of host plants by resolving conflicting information and developing reliable means of diagnosis. *Plant and Soil*. 2009; 320:37-77

Brookes P, Powlson D, Jenkinson D. Measurement of microbial biomass phosphorus in soil. *Soil Biology and Biochemstry*. 1982; 14:319-329

Brookes PC, Landman A, Pruden G, Jenkinson DS. Chloroform fumigation and the release of soil nitrogen: a rapid direct extraction method to measure microbial biomass nitrogen in soil. *Soil Biology and Biochemistry*. 1985; 17:837-842

Calvo-Rodriguez S, Kiese R, Sánchez-Azofeifa GA. Seasonality and budgets of soil greenhouse gas emissions from a tropical dry forest successional gradient in Costa Rica. *Journal of Geophysical Research: Biogeosciences*. 2020; 125, e2020JG005647.

Camenzind T, Hättenschwiler S, Treseder KK, Lehmann A, Rillig MC. Nutrient limitation of soil microbial processes in tropical forests. *Ecological Monographs*. 2018; 88:4-21

Campbell EE, Paustian K. Current developments in soil organic matter modeling and the expansion of model applications: a review. *Environmental Research Letters*. 2015; 10:123004-123037

Campo J. Shifts from ecosystem P to N limitation at precipitation gradient in tropical dry forests at Yucatan, Mexico. 2016; *Environmental Research Letters.* 11: 095006

Chadwick O, Derry LA, Vitousek P, Huebert B, Hedin L. Changing sources of nutrients during four million years of ecosystem development. *Nature.* 1999; 397:491-497. 10.1038/17276.

Cleveland C, Liptzin D. C: N: P stoichiometry in soil: is there a "Redfield ratio" for the microbial biomass? *Biogeochemistry*. 2007; 85:235-252

Cleveland C, Townsend A, Taylor P, et al. Relationships among net primary productivity, nutrients and climate in tropical rain forest: a pan-tropical analysis. *Ecology Letters*. 2011; 14:939-947.

Cornelissen J, Aerts R, Carabolini B, Werger M, van der Heijden M. Carbon cycling traits of plant species are linked with mycorrhizal strategy. *Oecologia.* 2001; 129:611-619

Corrales A, Henkel TW, Smith ME. Ectomycorrhizal associations in the tropics – biogeography, diversity patterns, and ecosystem roles. *New Phytologist*. 2018; 220: 1076-1091

Corrales A, Mangan SA, Turner BL, Dalling JW. An ectomycorrhizal nitrogen economy facilitates monodominance in a neotropical forest. *Ecology Letters.* 2016; 19: 383–392

Cotler H, Ortega-Larrocea MP. Effects of land use on soil erosion in a tropical dry forest ecosystem, Chamela watershed, Mexico. *Catena.* 2006; 65:107–117.

Cotrufo MF, Wallenstein MD, Boot CM, Denef K, Paul E. The Microbial Efficiency-Matrix Stabilization (MEMS) framework integrates plant litter decomposition with soil organic matter stabilization: do labile plant inputs form stable soil organic matter? *Global Change Biology*. 2013; 19:988-995

Cross AF, Schlesinger WH. A literature review and evaluation of the Hedley fractionation: Applications to the biogeochemical cycle of soil phosphorus in natural ecosystems. *Geoderma.* 1995: 64:197-214.

Eamus D. Ecophysiological traits of deciduous and evergreen woody species in the seasonally dry tropics. *Trends in Ecology and Evolution*. 1999; 14:11-16.

Elser JJ, Dobberfuhl DR, MacKay NA, Schampel JH. Organism size, life history, and N:P stoichiometry: toward a unified view of cellular and ecosystem processes. *Bioscience*. 1996; 46: 674-684

Ettema CH, Wardle DA. Spatial soil ecology. *Trends in Ecology and Evolution.* 2002; 17:177-183

Feng X, Porporato A, Rodriguez-Iturbe I. Changes in rainfall seasonality in the tropics. *Nature Climate Change.* 2013; 3:811-815

Fernandez CW, Kennedy PG. Revisiting the "Gadgil effect": do interguild fungal interactions control carbon cycling in forest soils? *New Phytologist* 2016; 209:1382-1394

Fleischer K, Rammig A, De Kauwe M, Walker AP, Domingues TF, Fuchslueger L, *et al.* Amazon forest response to CO2 fertilization dependent on plant phosphorus acquisition. *Nature Geoscience*. 2019; 12:736-741

Frahm, E., G.F. Monnier, N.A. Jelinski, E. Fleming, B.L. Barber, R.A. Knurr, J.B. Lambon. Chemical Soil Surveys at the Bremer Site (Dakota County, Minnesota, USA): Measuring Phosphorous Content of Sediment by Portable XRF and ICP-OES. *Journal of Archaeological Science. 2016;* 75: 115-138.

Frey SD, Lee J, Melillo JM, Six J. The temperature response of soil microbial efficiency and its feedback to climate. *Nature Climate Change*. 2013; 3:395-398

Friedlingstein P, Meinshausen M, Arora VK, et al. Uncertainties in CMIP5 climate projections due to carbon cycle feedbacks. *Journal of Climate*. 2014; 27:511-526

Frioni L, Minasian H, and Volfovicz R. Arbuscular mycorrhizae and ectomycorrhizae in native tree legumes in Uruguay. *Forest Ecology and Management.* 1999; 115:41-47

Galicia L, Garcia-Oliva F. The effects of C, N and P additions on soil microbial activity under two remnant tree species in a tropical seasonal pasture. *Applied Soil Ecology*. 2004; 26:31-39

Gamboa AM, Hidalgo C, De Leon F, Etchevers JD, Gallardo JF, Campo J. Nutrient addition differentially affects soil carbon sequestration in secondary tropical dry forests: early- versus late-succession stages. *Restoration Ecology.* 2010; 18: 252–260

Gei MG, Powers JS. The influence of seasonality and species effects on surface fine roots and nodulation in tropical legume tree plantations. *Plant and Soil.* 2015; 388:187-196

Gei MG, Powers JS. 2014. Nutrient cycling in tropical dry forests. pp 141-155 *in* Sanchez-Azofeifa GA, Powers JS, Fernandes GW, Quesada M, eds. Tropical Dry Forests in the Americas: Ecology, Conservation, and Management. CRC Press, Boca Raton FL.

Goll D, Vuichard N, Maignan F, Jornet-Puig A, Sardans J, Violette A, *et al.* A representation of the phosphorus cycle for ORCHIDEE (revision 4520). *Geoscientific Model Development Discussions*. 2017; 10:3745-2770

Gu C, Dam T, Hart SC, Turner BL, Chadwick OA, Berhe AA, Hu Y, Zhu M. Quantifying uncertainties in sequential chemical extraction of soil phosphorus using XANES specroscopy. *Environ Sci Technol*. 2020; 54: 2257-2267.

Gutknecht JLM Field CB, Balser TC. Microbial communities and their responses to simulated global change fluctuate greatly over multiple years. *Global Change Biology.* 2012; 18: 2256–69

Hartman WH, Richardson CJ. Differential nutrient limitation of soil microbial biomass and metabolic quotients (qCO_2): is there a biological stoichiometry of soil microbes? *PLoS One.* 2013; 8:357127

Hedley MJ, Steward JWB, Chauhan BS. Changes in inorganic and organic soil phosphorus fractions induced by cultivation practices and by laboratory incubations. *Soil Science Society of America Journal.* 1982; 46: 970-976

Hogberg MN, Hogberg P. Extramatrical ectomycorrhizal mycelium contributes one-third of microbial biomass and produces, together with associated roots, half the dissolved organic carbon in a forest soil. *New Phytologist.* 2002; 154: 791-795

Hulshof CM, Powers JS. Tropical forest composition and function across space and time: Insights from diverse gradients in Área de Conservación Guanacaste. *Biotropica.* 2019; DOI: 10.1111/btp.12689

Hulshof CM, Swenson NG. Variation in leaf functional trait values within and across individuals and species: an example from a Costa Rican dry forest. *Functional Ecology.* 2010; 24:217-223

Jackson ML, Lim CH, Zelazny LW. Oxides, hydroxides, and aluminosilicates. *In* A. Klute (ed.) Methods of Soil Analysis. Part 1. Physical and Mineralogical Methods. 2nd ed. *Agronomy*. 1997; 9:101–150.

Jackson RB, Lajtha K, Crow SE, Hugelius G, Kramer MG, Piñeiro G. The ecology of soil carbon: Pools, vulnerabilities, and biotic and abiotic controls. *Annu Rev Ecol Evol Syst*. 2017; 48:419-445

Jenny H. Factors of soil formation: a system of quantitative pedology. 1941; Dover Publications, New York NY.

Jha CS, Singh JS. Composition and dynamics of dry tropical forest in relation to soil texture. *Journal of Vegetation Science.* 1990; 1:609-614

John R, Dalling J, Harms K, et al. Soil nutrients influence spatial distributions of tropical tree species. *Proceedings of the National Academy of Sciences*. 2007; 104:864-869.

Jungerius PD. Quaternary landscape development of the Río Magdalena Basin between Neiva and Bogotá (Colombia). *Palaeogeography, Palaeoclimatology, Palaeoecology.* 1976; 19: 89-137.

Keeney DR, Nelson DW. 1987. Nitrogen: inorganic forms. pp.648-649. In Page AL et al., eds., Methods of Soil Analysis: Part 2, Chemical and Microbiological Properties. Soil Science Society of America, Madison, Wisconsin USA

Konert M, Vandenberghe J. Comparison of laser grain size analysis with pipette and sieve analysis: a solution for the underestimation of the clay fraction. *Sedimentology.* 1997; 44: 523–535.

Kuzyakov Y, Blagodatskaya E. Microbial hot spots and hot moments in soil: Concept and review. *Soil Biology and Biochemistry.* 2015; 83:184-199

Lado-Monserrat L, Lull C, Bautista I, Lidón A, Herrera R. Soil moisture increment as a controlling variable of the "Birch effect:" Interactions with the pre-wetting soil moisture and litter addition. *Plant Soil*. 2014; 379:21-34

Levy-Varon JH, Batterman SA, Medvigy D, Xu X, Hall JS, van Breugel M, Hedin LO. Tropical carbon sink accelerated by symbiotic dinitrogen fixation. *Nature Communications.* 2019; 10:5637

Liang C, Schimel JP, Jastrow JD. The importance of anabolism in microbial control over soil carbon storage. *Nature Microbiology*. 2017; 2:17105

Lugo AE, Medina E, Trejo Torres JC. Botanical and ecological basis for the resilience of Antillean dry forests. In: Pennington RT, Lewis GP, Ratter JA, editors. Neotropical savannas and seasonally dry forests: Plant diversity, biogeography, and conservation. 2006; Taylor and Francis Group, Boca Raton, FL

Manzoni S, Porporato A. Soil carbon and nitrogen mineralization: Theory and models across scales. *Soil Biology and Biochemistry*. 2009; 41:1355-1379

Margenot AJ, Paul BK, Sommer RR, Pulleman MM, Parikh SJ, Jackson LE, Fonte SJ. Can conservation agriculture improve phosphorus (P) availability in weathered soils? Effects of tillage and residue management on soil P status after 9 years in a Kenyan Oxisol. *Soil and Tillage Research*. 2017; 166: 157-166.

McGill W, Cole C. Comparative aspects of cycling of organic C, N, S and P through soil organic matter. *Geoderma*. 1981; 26:267-286

McGuire KL, Zak DR, Edwards IP, Blackwood CB, Upchurch R. Slowed decomposition is biotically mediated in an ectomycorrhizal, tropical rain forest. *Oecologia.* 2010; 164:785-795.

Medvigy D, Wang G, Zhu Q, et al. Observed variation in soil properties can drive large variation in modeled forest functioning and composition during tropical forest secondary succession. *New Phytologist.* 2019; DOI:10.1111/nph.15848

Miller BA, Schaetzl RJ. Precision of soil sample particle size results using laser diffractometry. Soil Science Society of America Journal. 2012;76 1719 - 1727

Moore JAM, Jiang J, Patterson CM, Mayes MA, Wang G, Classen AT. Interactions among roots, mycorrhizas and free-living microbial communities differentially impact soil carbon processes. *Journal Ecology*. 2015; 103:1442-1453

Mooshammer M, Wanek W, Hammerle I, et al. Adjustment of microbial nitrogen use efficiency to carbon:nitrogen imbalances regulates soil nitrogen cycling. *Nature Communications*. 2014; 5:1-7

Murphy PG, Lugo A. Ecology of tropical dry forest. *Annu Rev Ecol Syst*. 1986; 17:67-88

Murphy J, Riley JP. A modified single solution method for the determination of phosphate in natural waters. *Ana Chim Acta.* 1962; 27: 31-36

Oksanen J, Blanchet FG, Friendly M, Kindt R, Legendre P, McGlinn D. vegan: Community ecology package. R package version 2.5-4. 2019; R Foundation for Statistical Computing

Oleson KW, Lawrence DW, Bonan GB, *et al*. Technical description of version 4.5 of the Community Land Model (CLM), NCAR/TN-503+STR, NCAR Technical Note. 2013.

Olson DM, Dinerstein E, Wikramanayake ED, Burgess ND, Powell GV, et al. Terrestrial Ecoregions of the World: A New Map of Life on Earth: A new global map of terrestrial ecoregions provides an innovative tool for conserving biodiversity. *BioScience*. 2001; 51; 933-938.

Orwin K, Kirschbaum M, St John M, Dickie I. Organic nutrient uptake by mycorrhizal fungi enhances ecosystem carbon storage: a model-based assessment. *Ecology Letters*. 2011; 14:493-502

Peñuelas J, Ciais P, Canadell JG, Janssens I, Fernandez-Martinez M, Jofre C, *et al.* Shifting from a fertilization-dominated to a warming-dominated period. *Nature Ecology & Evolution*. 2017; 1:1438-1445

Phillips R, Brzostek E, Midgley M. The mycorrhizal-associated nutrient economy: a new framework for predicting carbon–nutrient couplings in temperate forests. *New Phytologist*. 2013; 199:41-51

Powers J, Tiffin P. Plant functional type classifications in tropical dry forests in Costa Rica: leaf habit versus taxonomic approaches. *Functional Ecology*. 2010; 24:927-936

Powers J, Becknell J, Irving J, Perez-Aviles D. Diversity and structure of regenerating tropical dry forests in Costa Rica: Geographic patterns and environmental drivers. *Forest Ecology and Management*. 2009a; 258:959-970

Powers JS, Montgomery RA, Adair EC, et al. Decomposition in tropical forests: a pan-tropical study of the effects of litter type, litter placement and mesofaunal exclusion across a precipitation gradient. *Journal of Ecology*. 2009b; 97:801-811

Powers JS, Corre MD, Twine TE, Veldkamp E. Geographic bias of field observations of soil carbon stocks with tropical land-use changes precludes spatial extrapolation. *Proceedings of the National Academy of Sciences* 2011; 108(15) 6318-6322.

Pulla S, Riotte J, Suresh HS, Dattaraja HS, Sukumar R. Controls of soil spatial variability in a dry tropical forest. *PLoS One.* 2016; 11:e0153212

Rasmussen C, Heckman K, Wieder WR, et al. Beyond clay: towards an improved set of variables for predicting soil organic matter content. *Biogeochemistry*. 2018; 137:297-306

Rasse D, Rumpel C, Dignac MF. Is soil carbon mostly root carbon? Mechanisms for a specific stabilisation. *Plant Soil*. 2005; 269:341-356

Reed SC, Yang X, Thornton PE. Incorporating phosphorus cycling into global modeling efforts: a worthwhile, tractable endeavor. *New Phytologist*. 2015; 2018: 324-329

Rentería LY, Jaramillo VJ. Rainfall drives leaf traits and leaf nutrient resorption in a tropical dry forest in Mexico. *Oecologia.* 2011; 165:201-211

Robertson GP, Klingensmith KM, Klug MJ, Paul EA, Crum JA, Ellis BG. 1997. Soil resources, microbial activity, and primary production across an agricultural ecosystem. *Ecol. Appl.* 1997; 7:158-170.

Rosseel Y. *lavaan*: An R package for structural equation modeling. *Journal of Statistical Software*. 2012; 48: 1–36

Saiya-Cork KR., Sinsabaugh RL, Zak DR. The effects of long term nitrogen deposition on extracellular enzyme activity in an Acer saccharum forest soil. *Soil Biology and Biochemistry*. 2002; 34:1309–1315.

Sheffer E, Batterman SA, Levin SA, Hedin LO. Biome-scale nitrogen fixate strategies selected by climatic constraints on nitrogen cycle. *Nature Plants.* 2015; 1:15182

Schilling EM, Waring BG, Schilling JS, Powers JS. Forest composition modifies litter dynamics and decomposition in regenerating tropical dry forest. *Oecologia*. 2016; 182: 287-297

Schwartz NB, Lintner B, Feng S, Powers JS. Beyond MAP: A guide to rainfall seasonality for tropical ecologists. *In revision*, Biotropica.

Schwertmann U, Taylor RM. Iron oxides. *In* J.B. Dixon and S.B. Weed (eds.) Minerals in the Soil Environment. 2nd ed. Soil Science Society of America. 1989; 1:370– 438.

Shah F, Nicolás C, Bentzer J, et al. Ectomycorrhizal fungi decompose soil organic matter using oxidative mechanisms adapted from saprotrophic ancestors. *New Phytologist*. 2016; 209:1705-1719

Singh J, Raghubanshi A, Singh R, Srivastava S. Microbial biomass acts as a source of plant nutrients in dry tropical forest and savanna. *Nature*. 1989; 338:499-500

Sinsabaugh R, Follstad Shah J. Ecoenzymatic stoichiometry and ecological theory. *Annu Rev Ecol Evol Syst*. 2012; 43:313-343

Sinsabaugh R, Manzoni S, Moorhead D, Richter A. Carbon use efficiency of microbial communities: stoichiometry, methodology and modelling. *Ecology Letters*. 2013; 16:930-939

Sistla SA, Schimel JP. Stoichiometric flexibility as a regulator of carbon and nutrient cycling in terrestrial ecosystems under change. *New Phytologist*. 2012; 196:68-78

Smith-Martin CM, Xu X, Medvigy D, Schnitzer SA, Powers JS. Allometric scaling laws linking biomass and rooting depth vary across ontogeny and functional groups in tropical dry forest lianas and trees. *New Phytologist.* 2019; DOI: 10.111/nph.16725

Soil Survey Staff. 2014. Kellogg Soil Survey Laboratory Methods Manual. Soil Survey Investigations Report No. 42, Version 5.0. R. Burt and Soil Survey Staff (ed.). USDA Natural Resources Conservation Service.

Solís E, Campo J. Soil N and P dynamics in two secondary tropical dry forests after fertilization. *Forest Ecology and Management*. 2004; 195:409–418

Strickland M, Rousk J. Considering fungal: bacterial dominance in soils-Methods, controls, and ecosystem implications. *Soil Biol Biochem*. 2010;42:1385-1395.

Sullivan B, Smith W, Townsend A, et al. Spatially robust estimates of biological nitrogen (N) fixation imply substantial human alteration of the tropical N cycle. *Proceedings of the National Academy of Sciences*. 2014;111:8101-8106

Sulman BN, Brzostek ER, Medici C, Shevliakova E, Menge DNL, Phillips RP. Feedbacks between plant N demand and rhizosphere priming depend on type of mycorrhizal association. *Ecology Letters*. 2017; 20:1043-1053

Terrer C, Jackson RB, Prentice IC, et al. Nitrogen and phosphorus constrain the CO_2 fertilization of global plant biomass. *Nature Climate Change*. 2019; 9:684-689

Thum T, Caldararu S, Engel J, Kern M, Pallandt M, Schnur R, *et al.* A new terrestrial biosphere model with coupled carbon, nitrogen, and phosphorus cycles (QUINCY v1.0; revision 1772). *Geoscientific Model Development Discussions*. 2019; DOI: 10.5194/gmd-2019-49

Townsend AR, Asner GP, Cleveland CC. The biogeochemical heterogeneity of tropical forests. *Trends in Ecology and Evolution*. 2008; 23:424-431

Van Bodegom PM, Douma JC, Witte JPM, Ordoñez JC, Bartholomeus RP, Aerts R. Going beyond limitations of plant functional types when predicting global ecosystem-atmosphere fluxes: exploring the merits of trait-based approaches. *Global Ecology and Biogeography*. 2012; 21:625-636

Verduzco VS, Garatuza-Payán J, Yépez EA, Watts CJ, Rodríguez JC, Robles-Morua A, Vivoni ER. Variations of net ecosystem production due to seasonal precipitation differences in a tropical dry forest of northwest Mexico. *Biogeosciences*. 2015; 120:2081-2094

Walker T, Syers J. The fate of phosphorus during pedogenesis. *Geoderma*. 1976; 15:1-19

Wang B, Qiu L. 2006. Phylogenetic distribution and evolution of mycorrhizas in land plants. *Mycorrhiza*. 2006; 16:299-363.

Waring BG, Averill C, Hawkes CV. Differences in fungal and bacterial physiology alter soil carbon and nitrogen cycling: insights from meta-analysis and theoretical models. *Ecology Letters*. 2013; 16:887-894

Waring B, Becknell J, Powers J. Nitrogen, phosphorus, and cation use efficiency in stands of regenerating tropical dry forest. *Oecologia*. 2015; 178:887-897

Waring BG, Adams R, Branco S, Powers JS. Scale-dependent variation in nitrogen cycling and soil fungal communities along gradients of forest composition and age in regenerating tropical dry forests. *New Phytologist*. 2016; 209:845-854

Waring BG, Powers JS. Unraveling the mechanisms underlying pulse dynamics of soil respiration in tropical dry forests. *Environmental Research Letters*. 2016; 11:105005

Waring BG, Powers JS. Overlooking what is underground: Root:shoot ratios and coarse root allometric equations for tropical forests. *Forest Ecology and Management*. 2017; 385:10-15

Waring BG, Peréz Aviles D, Murray JG, Powers JS. Plant community responses to stand-level nutrient fertilization in a secondary tropical dry forest. *Ecology*. 2019; 100:e02691

Waring, B., et al. 2021. Soil biogeochemistry across Central and South American tropical dry forests. Dryad, data set. https://doi.org/10.5061/dryad.v15dv41vf

Weintraub SR, Taylor PG, Porder S, Cleveland CC, Asner GP, Townsend AR. Topographic controls on soil nitrogen availability in a lowland tropical forest. *Ecology*. 2015; 96:1561-1574

Werden LK, Becknell JM, Powers JS. Edaphic factors, successional status and functional traits drive habitat associations of trees in naturally regenerating tropical dry forests. *Functional Ecology.* 2018; 32:2766-2776

West AJ, Galy A, Bickle M. Tectonic and climatic controls on silicate weathering. *Earth and Planetary Science Letters.* 2005; 235: 211-218

Wieder WR, Cleveland CC, Smith WK, Todd-Brown K. Future productivity and carbon storage limited by terrestrial nutrient availability. *Nature Geoscience*. 2015; 8:441-444.

Wilson SW, Lambert JJ, Nanzyo M, Dahlgren RA. Soil genesis and mineralogy across a volcanic lithosequence. *Geoderma.* 2017; 285: 301-312.

Wullschleger SD, Epstein HE, Box EO, et al. Plant functional types in Earth system models: past experiences and future directions for application of dynamic vegetation models in high-latitude ecosystems. *Annals of Botany*. 2014; 114:1-16

Wurzburger N, Hedin LO. Taxonomic identity determines N_2 fixation by canopy trees across lowland tropical forests. *Ecology Letters.* 2016; 19:62-70

Yang X, Ricciuto DM, Thornton PE, Shi X, Xu M, Hoffman F, Norby RJ. The effects of phosphorus cycle dynamics on carbon sources and sinks in the Amazon region: a modeling study using ELM v1. *Journal of Geophysical Research: Biogeosciences.* 2019; DOI: 10.1029/2019JG005082

Yu L, Ahrens B, Wutzler T, Schrumpf M, Zaehle S. Jena Soil Model: a microbial soil organic carbon model integrated with nitrogen and phosphorus processes. *Geoscientific Model Development Discussions.* 2019; DOI: 10.5194/gmd-2019-187

Zhang J, Elser JJ. Carbon:nitrogen:phosphorus stoichiometry in fungi: a meta-analysis. *Frontiers in Microbiology.* 2017; DOI: 10.3389/fmicb.2017.01281

Zhu Q, Riley WJ, Tang J, Koven CD. Multiple soil nutrient competition between plants, microbes, and mineral surfaces: model development, parameterization, and example applications in several tropical forests. *Biogeosciences.* 2016; 13:341-363

Zhu Q, Riley WJ, Tang J, Collier N, Hoffman FM, Yang X, Bisht G. Representing nitrogen, phosphorus, and carbon interactions in the E3SM Land Model: Development and global benchmarking. *Journal of Advances in Modeling Earth Systems.* 2019; 11:2238-2258

Zinke PJ. The pattern of influence of individual forest trees on soil properties. *Ecology*. 1962; 43:130-133

Table 1. Climatic profiles and plant community characteristics for each of the 16 study plots arrayed across four tropical dry forest sampling sites. Abbreviations: mean annual temperature (MAT); mean annual precipitation (MAP); seasonality index (SI); ectomycorrhizal tree species (ECM).

Site and soil type	MAT (°C)	MAP (mm)	SI*	No. dry mos	Plot	Stand age (y)	Dominant species**	% legume basal area†	% ECM basal area†
Colombia (CO); Recent alluvial sediments that cover tuff	28	1833	0.17	4.3	CO_A	~50	Trichilia acuminata Coccoloba obtusifolia Machaerium capote	6.4	7.5
					CO_B	~50	Trichilia acuminata Eugenia procera Astronium graveolens	1.2	0.4
					CO_C	~50	Trichilia acuminata Oxandra espintana Coccoloba obtusifolia	0.2	14.1
					CO_D	~50	Trichilia acuminata Machaerium capote Astronium graveolens	12.2	0.2
Costa Rica (CR); Inceptisol (Andic/ Typic Haplustept)	25	1761	0.52	6.6	CR_D	~30	Hymenaea courbaril Albizia saman Guazuma ulmifolia	53.4	4.9
					CR_E	~30	Enterolobium cyclocarpum Guazuma ulmifolia Cupania guatemalensis	50.0	8.7
					CR_I	~30	Guazuma ulmifolia Cupania guatemalensis Cedrela odorata	4.8	10.1
					CR_P	~30	Guazuma ulmifolia Hymenaea courbaril Allophylus racemosus	17.4	3.6
Mexico (MX);	27	1204	0.38	7.7	MX_A	16	Caesalpinia gaumeri Diphysa carthagenensis	64.5	1.9

Mollisol (Lithic Haplustoll)							Neomillspaughia emarginata		
					MX_B	23	Mimosa bahamensis Neomillspaughia emarginata Bauhinia ungulata	58.4	0.8
					MX_C	33	Bursera simaruba Mimosa bahamensis Cochlospermum vitifolium	22.8	4.6
					MX_D	80	Bursera simaruba Neomillspaughia emarginata Diospyros anisandra	16.8	10.2
Puerto Rico (PR); Mollisol (Aridic/ Typic Calciustoll)	25	825	0.29	10.4	PR_HH	80	Swietenia mahagoni Amyris elemifera Coccoloba diversifolia	6.4	6.1
					PR_LL	>100	Gymnanthes lucida Bursera simaruba Pisonia albida	12.3	21.0
					PR_M1	>100	Pictetia aculeata Gymnanthes lucida Bourreria baccata	15.8	8.6
					PR_M2	>100	Gymnanthes lucida Coccoloba microstachya Pisonia albida	4.0	33.5

* Seasonality index calculated following Feng et al. (2013) as $S = D \bullet R/R_{max}$, where R and Rmax are observed and maximum annual rainfall, and D is concentration of rainfall in the wet season (higher values of *S* indicate greater seasonality)

** Based on percentage basal area of each species

† Dominance of legume and ectomycorrhizal (ECM) tree species, as a percentage of total basal area of stems ≥ 5 cm diameter at breast height. Ectomycorrhizal hosts were identified from Frioni et al. (1999), Wang and Qiu (2006), and Brundrett (2009).

Table 2. Derived variables included in multiple regression and path analyses to explore climatic, edaphic, and ecological controls on C, N, and P cycling.

Derived variable	**Constituent variables**	**Method of derivation**
C and N cycling	total organic C and N, microbial biomass C and N, NAG activity	First axis of PCA on core dataset*
P cycling	P_{labile}, microbial biomass P, F:B	Second axis of PCA on core dataset*
MAP	Total annual rainfall at each site	
Soil elemental composition	Total concentrations of Al, Ca, Fe, S	First axis of PCA on soil element concentrations measured with pXRF
Soil weathering status	Total concentrations of K, P, Si; ratio of Fe_{CD}:Fe	Second axis of PCA on soil element concentrations measured with pXRF
Plant community structure	presence/absence of plant species across plots	Second axis** of NMDS on Bray-Curtis dissimilarity matrix
Plant aboveground biomass	tree basal area per ha of plot area	
Relative abundance of plant functional groups	percent basal area comprised by legumes or ectomycorrhizal trees	

* The core dataset consists of: total organic nutrients (TOC, TN, $P_{organic}$); microbial biomass C, N, and P; inorganic nutrients (NH_4, NO_3, P_{labile}); enzymes (BG, NAG, AP, PPO, PER); F:B.

** First NMDS axis not included in subsequent analyses due to high collinearity with other predictor variables (VIF > 11)

Table 3. Plot-level means and standard errors for pH, soil moisture (SM), soil clay content (Clay), and C, N, and P pools. Abbreviations: total organic C (TOC); total nitrogen (TN); organic and labile P pools (P_{org}, P_{labile}); soil moisture (SM); microbial biomass C, N, and P (MBC, MBN, MBP); dissolved organic N (DON). Plots are labeled by two letter site codes first, followed by site-specific plot identifiers.

Plot	pH	Clay (%)	TOC (%)	TN (%)	P_{org} μg g^{-1}	P_{labile} μg g^{-1}	Season	SM (%)	MBC μg g^{-1}	MBN μg g^{-1}	MBP μg g^{-1}	DON μg g^{-1}	PO_4 μg g^{-1}
CO A	6.3 ± 0.2	23.7 ± 1.3	3.5 ± 0.3	0.28 ± 0.04	116 ± 12	34.4 ± 3.6	dry	9 ± 1	813 ± 75	23 ± 5	10 ± 2	17.6 ± 3.7	1.5 ± 0.5
							wet	13 ± 1	902 ± 59	48 ± 3	17 ± 3	16.1 ± 2.9	4.3 ± 0.7
CO B	5.4 ± 0.2	21.8 ± 0.3	3.5 ± 0.3	0.27 ± 0.03	153 ± 23	47.9 ± 4.9	dry	6 ± 1	567 ± 11	19 ± 4	5 ± 3	19.7 ± 3.4	4.1 ± 1.3
							wet	9 ± 1	748 ± 29	38 ± 3	22 ± 10	24.2 ± 4.3	13.2 ± 1.6
CO C	6.0 ± 0.2	22.8 ± 1.6	2.9 ± 0.2	0.27 ± 0.03	134 ± 12	49.6 ± 2.8	dry	9 ± 1	746 ± 95	21 ± 6	13 ± 4	13.5 ± 2.0	3.0 ± 0.6
							wet	13 ± 1	1053 ± 96	56 ± 7	19 ± 9	15.0 ± 3.2	8.7 ± 1.6
CO D	5.9 ± 0.1	20.5 ± 1.3	3.1 ± 0.4	0.29 ± 0.04	90 ± 7	44.4 ± 2.6	dry	10 ± 1	815 ± 64	14 ± 3	5 ± 3	9.0 ± 1.8	4.5 ± 1.4
							wet	12 ± 1	1251 ± 73	38 ± 4	40 ± 6	9.0 ± 1.2	8.4 ± 2.0
CR D	5.8 ± 0.1	57.5 ± 0.7	2.8 ± 0.2	0.22 ± 0.01	94 ± 6	5.4 ± 1.0	dry	17 ± 1	817 ± 71	27 ± 4	1 ± 1	13.0 ± 1.0	1.5 ± 0.1
							wet	34 ± 1	110 ± 16	32 ± 4	3 ± 1	16.6 ± 1.5	1.2 ± 0.2
CR E	6.0 ± 0.1	44.7 ± 0.7	3.1 ± 0.2	0.27 ± 0.02	141 ± 13	3.0 ± 0.7	dry	21 ± 1	937 ± 94	32 ± 8	4 ± 2	17.0 ± 1.0	1.2 ± 0.3
							wet	37 ± 1	715 ± 212	76 ± 17	4 ± 2	27.2 ± 2.1	2.3 ± 0.6
CR I	6.3 ± 0.1	52.2 ± 1.1	3.8 ± 0.1	0.33 ± 0.01	169 ± 5	3.7 ± 0.3	dry	19 ± 1	859 ± 54	28 ± 7	4 ± 1	16.4 ± 0.9	0.6 ± 0.0
							wet	36 ± 1	568 ± 60	75 ± 10	12 ± 2	30.1 ± 2.4	2.4 ± 0.8
CR P	5.9 ± 0.1	45.3 ± 1.8	3.1 ± 0.2	0.27 ± 0.02	194 ± 23	8.1 ± 0.5	dry	16 ± 1	940 ± 70	40 ± 6	8 ± 3	11.3 ± 1.1	1.5 ± 0.9
							wet	38 ± 4	362 ± 35	43 ± 6	6 ± 1	16.9 ± 0.8	2.3 ± 0.1
MX A	6.6 ± 0.1	57.7 ± 2.1	4.8 ± 0.4	0.50 ± 0.02	154 ± 15	3.7 ± 1.1	dry	9 ± 2	1181 ± 59	25 ± 3	3 ± 1	21.7 ± 2.6	0.5 ± 0.1
							wet	29 ± 1	1651 ± 136	105 ± 8	16 ± 11	19.3 ± 1.2	1.9 ± 0.9

MX B	6.2 ± 0.1	53.0 ± 1.5	4.4 ± 0.5	0.36 ± 0.02	76 ± 3	1.3 ± 0.1	dry	14 ± 4	937 ± 102	30 ± 8	2 ± 1	20.2 ± 3.5	0.3 ± 0.1
							wet	30 ± 1	1278 ± 65	102 ± 7	2 ± 1	21.8 ± 1.2	2.1 ± 0.6
MX C	5.7 ± 0.1	47.2 ± 1.9	5.3 ± 0.4	0.49 ± 0.03	92 ± 2	1.6 ± 0.1	dry	11 ± 1	1135 ± 225	52 ± 15	3 ± 2	30.7 ± 7.1	0.4 ± 0.1
							wet	29 ± 1	1600 ± 166	122 ± 16	0 ± 0	24.6 ± 2.7	4.0 ± 0.3
MX D	6.5 ± 0.1	46.3 ± 3.0	4.8 ± 0.6	0.51 ± 0.06	80 ± 4	2.2 ± 0.4	dry	10 ± 1	1196 ± 220	54 ± 14	3 ± 2	41.2 ± 13.7	1.2 ± 0.8
							wet	31 ± 2	1600 ± 80	114 ± 11	4 ± 1	42.1 ± 9.5	1.6 ± 0.6
PR HH	7.3 ± 0.1	44.8 ± 0.9	8.1 ± 0.4	0.44 ± 0.02	150 ± 10	12.0 ± 3.2	dry	14 ± 1	1591 ± 103	81 ± 7	15 ± 6	21.9 ± 2.0	3.3 ± 0.4
							wet	19 ± 1	1960 ± 91	138 ± 4	4 ± 1	18.1 ± 1.7	10.0 ± 1.9
PR LL	7.2 ± 0.1	23.1 ± 4.3	22.1 ± 3.2	2.08 ± 0.27	204 ± 15	13.0 ± 2.1	dry	31 ± 5	4455 ± 821	280 ± 55	31 ± 10	233.0 ± 49.7	29.8 ± 5.2
							wet	50 ± 6	3855 ± 455	373 ± 30	111 ± 30	138.6 ± 20.1	133.5 ± 40.0
PR M1	7.2 ± 0.1	23.6 ± 1.2	8.5 ± 0.5	0.51 ± 0.02	101 ± 3	2.2 ± 0.3	dry	9 ± 1	1298 ± 152	81 ± 13	3 ± 3	19.6 ± 2.0	2.8 ± 0.4
							wet	19 ± 1	2230 ± 200	168 ± 24	45 ± 8	28.2 ± 2.5	6.5 ± 1.2
PR M2	7.1 ± 0.1	24.8 ± 1.5	17.6 ± 0.9	1.47 ± 0.05	162 ± 13	6.7 ± 1.7	dry	28 ± 2	4063 ± 452	250 ± 18	9 ± 2	123.2 ± 22.1	19.6 ± 5.6
							wet	46 ± 2	3800 ± 533	348 ± 45	56 ± 21	108.9 ± 16.8	42.5 ± 9.9

Table 4. F statistics for analyses of variance performed on biogeochemical variables measured at a single timepoint. Significant F values are shown in bold. Abbreviations: total organic C (TOC); total nitrogen (TN).

	pH	Clay	Silt	Sand	TOC	TN	$P_{i\text{-}AEM}$	$P_{o\text{-}H2O}$	$P_{i\text{-}bicarb}$	$P_{o\text{-}bicarb}$	$P_{i\text{-}NaOH}$	$P_{o\text{-}NaOH}$	$P_{i\text{-}HCl}$	P_{org}	P_{labile}
Site	**16.26**	**19.31**	**4.98**	**26.16**	**11.01**	**8.52**	**34.62**	**216.8**	**39.03**	**10.67**	**10.25**	0.99	**26.14**	1.97	**27.97**
Plot	**6.50**	**13.07**	**13.68**	**7.77**	**18.36**	**16.53**	**9.44**	**14.86**	**3.28**	**10.20**	**3.84**	**7.03**	**23.76**	**9.78**	**8.33**

Table 5. F statistics for analyses of variance performed on biogeochemical variables measured in both wet and dry seasons. Significant F values are shown in bold. Abbreviations: soil moisture (SM); microbial biomass C, N, and P (MBC, MBN, MBP); dissolved organic C and N (DOC, DON); net N mineralization rate (N_{min}); fungal:bacterial ratio (F:B).

	SM	MBC	DOC	MBN	N_{min}	DON	PO_4	MBP	BG	NAG	AP	PPO	PER	F:B
Site	**5.4**	**8.9**	**16.4**	**23.3**	**11.4**	**2.6**	**15.0**	**7.9**	1.0	**8.9**	1.4	**6.6**	**13.3**	**65.0**
Plot	**24.2**	**15.6**	**16.1**	**6.1**	**2.8**	**23.6**	**8.3**	1.6	**3.8**	**6.4**	**2.2**	1.2	1.0	**6.0**
Season	**347.2**	0.9	**8.7**	**128.4**	1.7	**10.5**	**95.4**	**14.4**	0.3	**5.0**	0.5	**6.4**	2.3	2.8
Site x Season	**24.5**	**4.6**	0.4	**6.0**	**5.4**	**2.8**	**2.9**	2.3	2.0	**5.6**	2.6	**7.7**	1.7	**6.0**

Figure Legends

Figure 1. Site-level means, averaged across seasons, for total organic C (TOC); microbial biomass C (MBC); dissolved organic C (DOC); total organic N (TN); microbial biomass N (MBN); the ratio of initial NH_4 to NO_3; total organic P (P_{org}); microbial biomass P (MBP); and labile P. Error bars are SE.

Figure 2. Proportion of variance explained by site, plot, season (where applicable), and the interaction between site and season. Results are presented for biogeochemical variables measured **A)** at one timepoint only vs. **B)** in both wet and dry seasons. 'Within-plot' variance is equal to residual variance. Abbreviations: TOC (total organic carbon); TN (total nitrogen); P_{org} (organic P); SM (soil moisture); fungi (abundance of fungal PLFAs); MBC, N, P (microbial biomass C, N, P); DOC, N (dissolved organic C and N).

Figure 3A) Abundance of fungal PLFAs across sites. **B)** Results of an NMDS analysis on soil PLFA profiles

Figure 4. Principal components analysis performed on soil biogeochemical variables. Only variables with loadings > 0.3 on at least one axis are shown: total organic C and N (TOC and TN); microbial biomass C, N, and P (MBC, MBN, MBP); labile inorganic P (P_{labile}) and the fungal:bacterial ratio (F:B). Note that a vector for NAG is not shown because it almost perfectly overlaps that of TN.

Figure 5. Path diagrams showing relationships between ecosystem state factors and **A**) an integrative C and N cycling index and **B**) a P cycling index. Only significant paths are shown. For path coefficients corresponding to each numbered arrow, see Appendix S1: Table S4. Confirmatory Fit Indices (CFI) and Root Mean Square Error of Approximation (RMSEA) are shown for each path model.

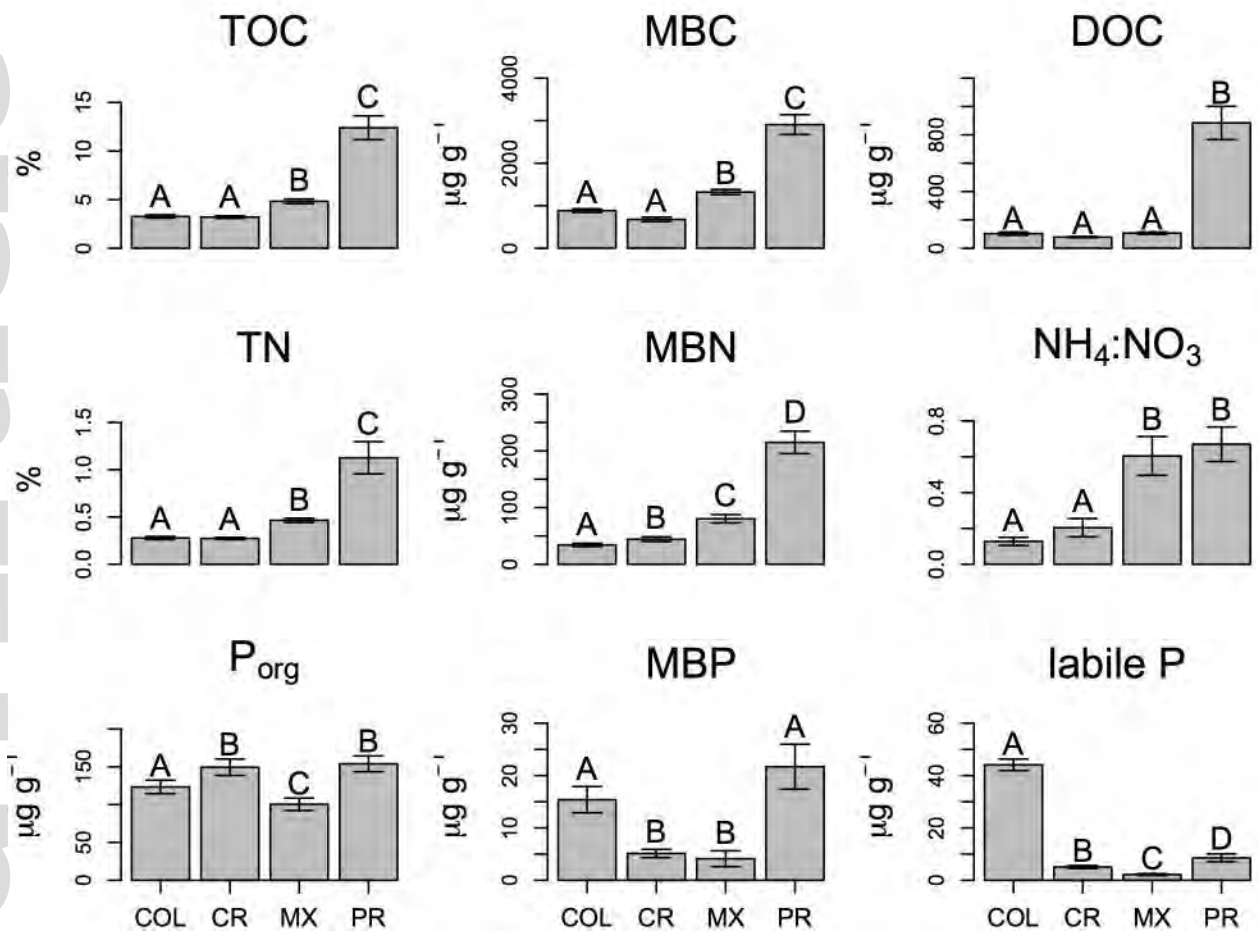

ecm_1453_f1.tiff

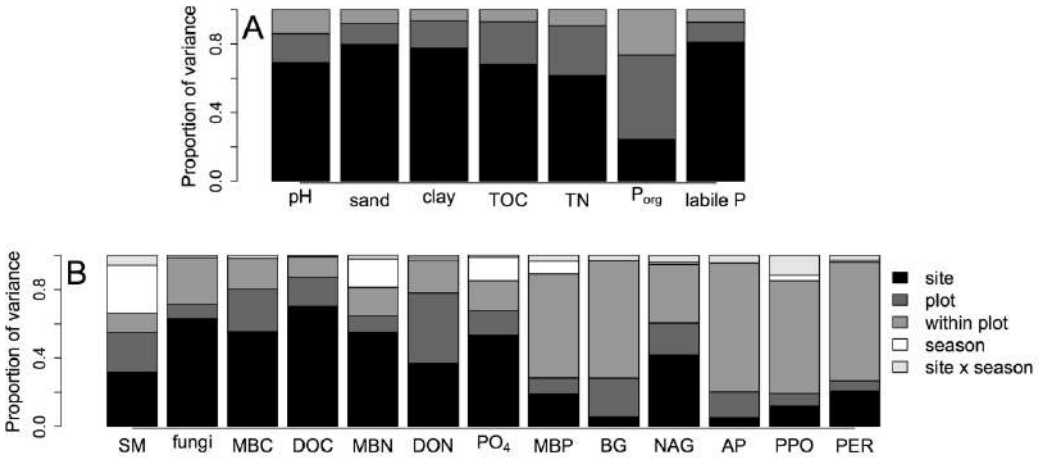

ecm_1453_f2.tiff

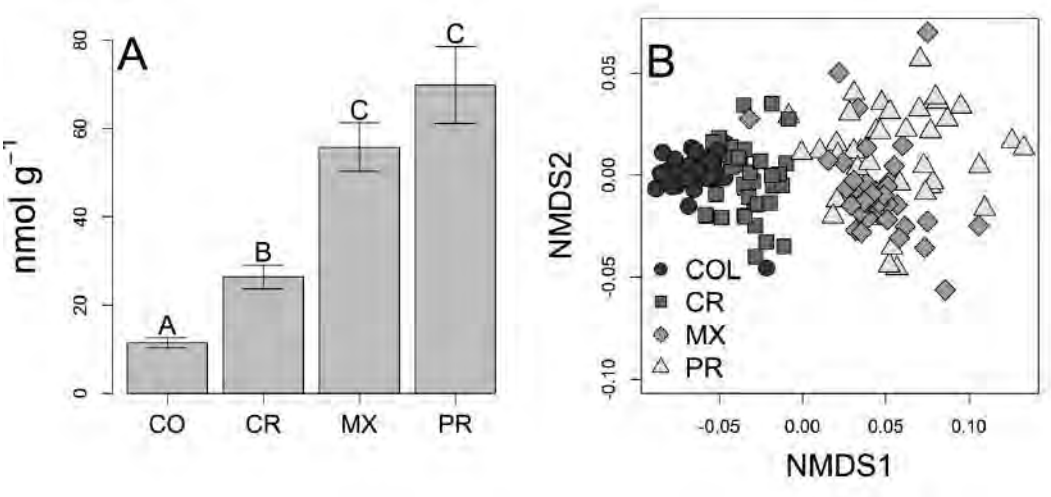

ecm_1453_f3.tiff

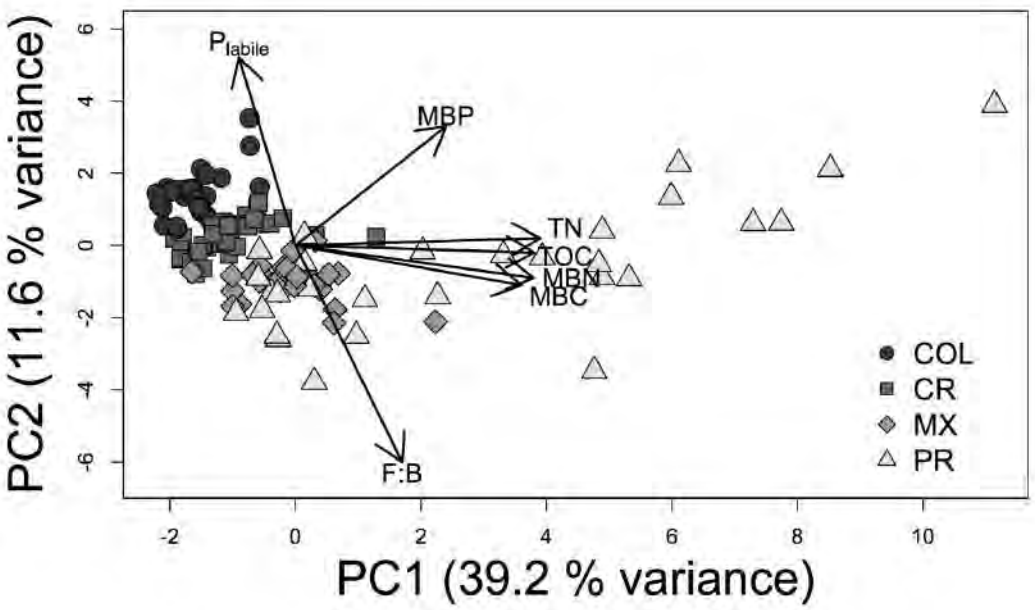

ecm_1453_f4.tiff

A

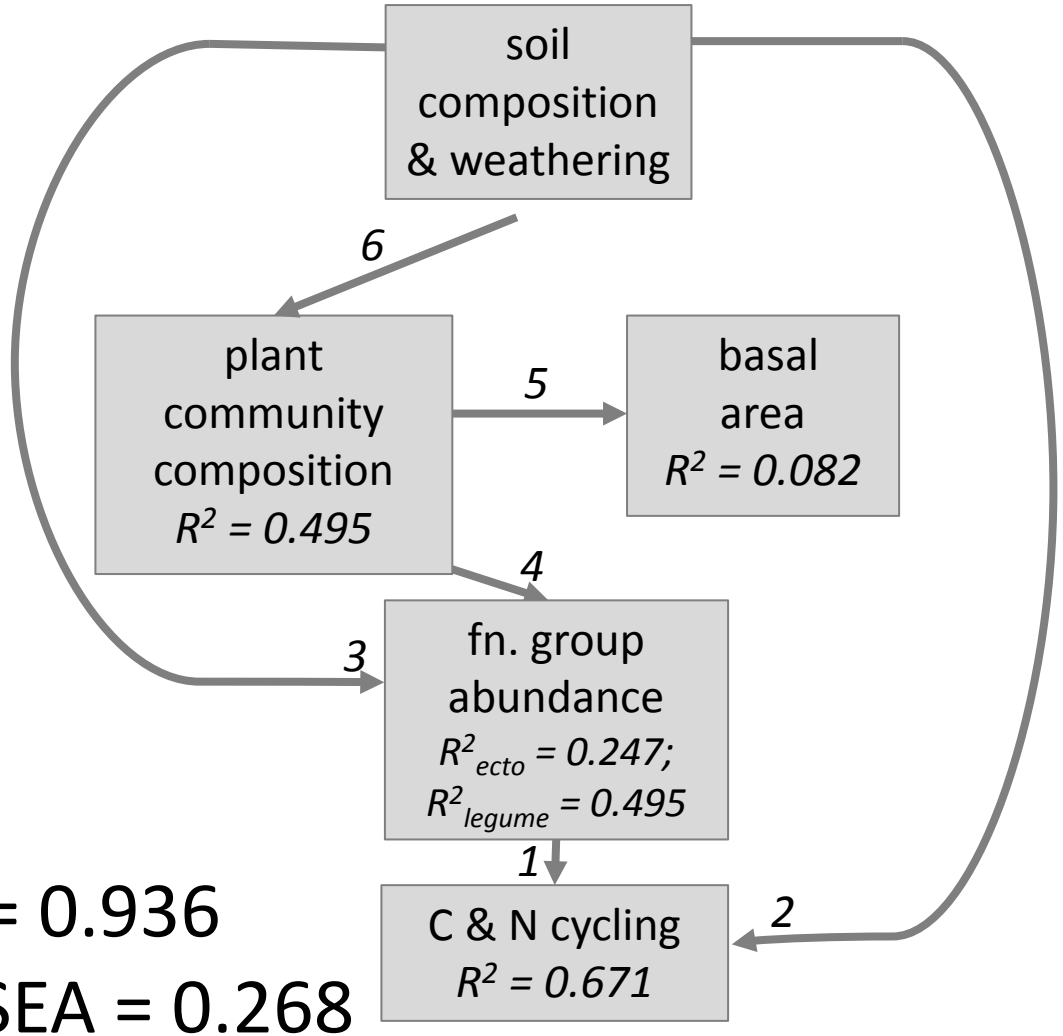

CFI = 0.936

RMSEA = 0.268

B

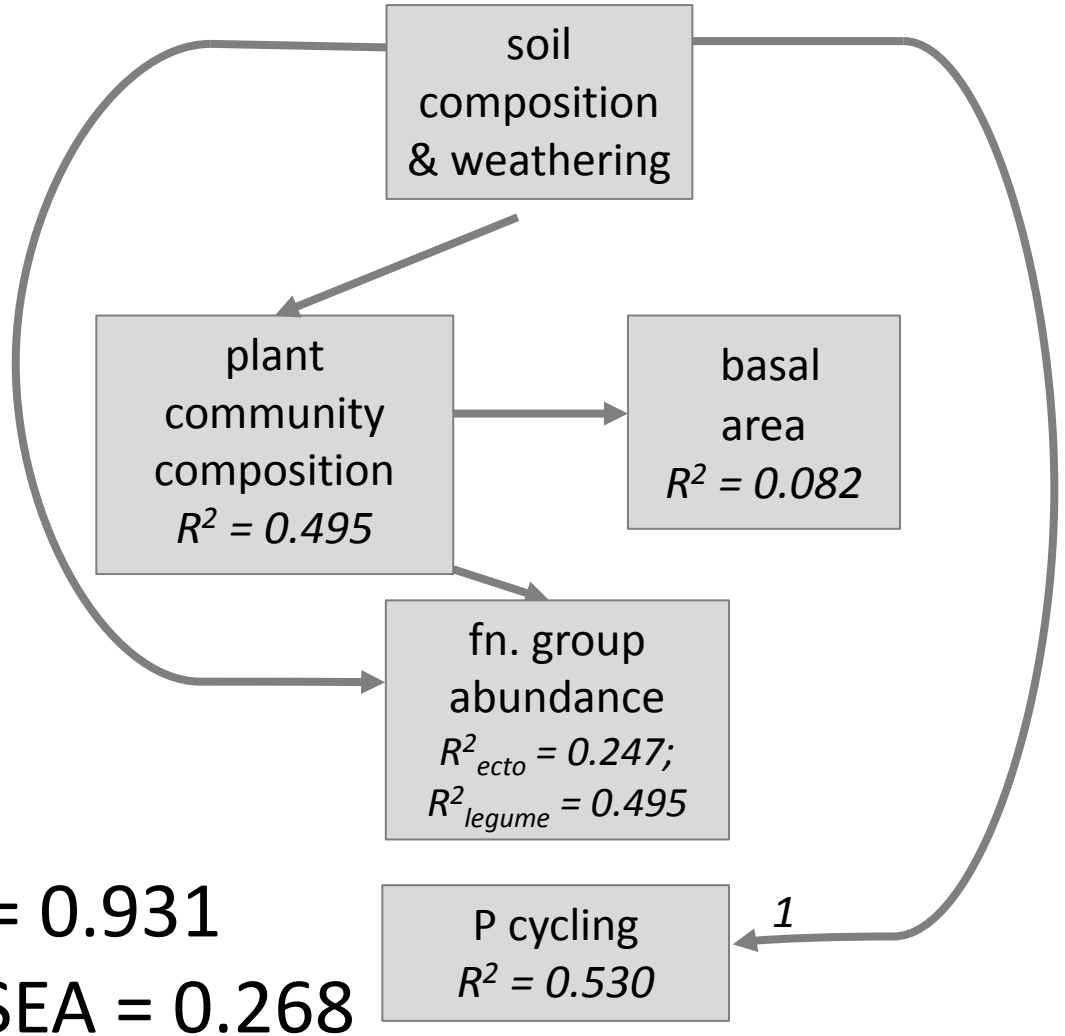

CFI = 0.931

RMSEA = 0.268